

Synthesis and NLO properties of new *trans* 2-(thiophen-2-yl)vinyl heteroaromatic iodides

Cosimo Gianluca Fortuna,^{a*} Carmela Bonaccorso^a, Fadi Qamar^b, Anu Anu^b, Isabelle Ledoux^b, Giuseppe Musumarra^a

SUPPORTING INFORMATION

Fig. S1. ^1H NMR spectrum of *N,N*-dibutyl-4-oxo-4-(2-thienyl)butanamide

Fig. S2. ^{13}C NMR spectrum of *N,N*-dibutyl-4-oxo-4-(2-thienyl)butanamide

Fig. S3. ^1H - ^1H gCOSY NMR spectrum of *N,N*-dibutyl-4-oxo-4-(2-thienyl)butanamide

Fig. S4. ^1H - ^{13}C gHSQCAD NMR spectrum of *N,N*-dibutyl-4-oxo-4-(2-thienyl)butanamide

Fig. S5. ^1H - ^{13}C gHMBCAD NMR spectrum of *N,N*-dibutyl-4-oxo-4-(2-thienyl)butanamide

Fig. S6. ^1H NMR spectrum of *N,N*-dibutyl-2,2'-bithiophen-5-amine

Fig. S7. ^{13}C NMR spectrum of *N,N*-dibutyl-2,2'-bithiophen-5-amine

Fig. S8. ^1H - ^1H gCOSY NMR spectrum of *N,N*-dibutyl-2,2'-bithiophen-5-amine

Fig. S9. ^1H - ^{13}C gHSQCAD NMR spectrum of *N,N*-dibutyl-2,2'-bithiophen-5-amine

Fig. S10. ^1H - ^{13}C gHMBCAD NMR spectrum of *N,N*-dibutyl-2,2'-bithiophen-5-amine

Fig. S11. ^1H NMR spectrum of 5'-(dibutylamino)-2,2'-bithiophene-5-carbaldehyde

Fig. S12. ^{13}C NMR spectrum of 5'-(dibutylamino)-2,2'-bithiophene-5-carbaldehyde

Fig. S13. ^1H NMR spectrum of 2-{(E)-2-[5'-(dibutylamino)-2,2'-bithien-5-yl]vinyl}-1-methylpyridinium iodide

Fig. S14. ^1H - ^1H gCOSY NMR spectrum of 2-{(E)-2-[5'-(dibutylamino)-2,2'-bithien-5-yl]vinyl}-1-methylpyridinium iodide

Fig. S15. ^1H - ^{13}C gHSQCAD NMR spectrum of 2-{(E)-2-[5'-(dibutylamino)-2,2'-bithien-5-yl]vinyl}-1-methylpyridinium iodide

Fig. S16. ^1H - ^{13}C gHMBCAD NMR spectrum of 2-{(E)-2-[5'-(dibutylamino)-2,2'-bithien-5-yl]vinyl}-1-methylpyridinium iodide

Fig. S17. ^1H NMR spectrum of 2- $\{(E)\text{-2-[5'-(dibutylamino)-2,2'-bithien-5-yl]vinyl}\}$ -1-methylquinolinium iodide

Fig. S18. ^{13}C NMR spectrum of 2- $\{(E)\text{-2-[5'-(dibutylamino)-2,2'-bithien-5-yl]vinyl}\}$ -1-methylquinolinium iodide

Fig. S19. ^1H - ^1H gCOSY NMR spectrum of 2- $\{(E)\text{-2-[5'-(dibutylamino)-2,2'-bithien-5-yl]vinyl}\}$ -1-methylquinolinium iodide

Fig. S20. ^1H - ^{13}C gHSQCAD NMR spectrum of 2- $\{(E)\text{-2-[5'-(dibutylamino)-2,2'-bithien-5-yl]vinyl}\}$ -1-methylquinolinium iodide

Fig. S21. ^1H - ^{13}C gHMBCAD NMR spectrum of 2- $\{(E)\text{-2-[5'-(dibutylamino)-2,2'-bithien-5-yl]vinyl}\}$ -1-methylquinolinium iodide

Fig. S22. ESI-MS spectrum of *N,N*-dibutyl-4-oxo-4-(2-thienyl)butanamide

Fig. S23. ESI-MS spectrum of *N,N*-dibutyl-2,2'-bithiophen-5-amine

Fig. S24. ESI-MS spectrum of 5'-(dibutylamino)-2,2'-bithiophene-5-carbaldehyde

Fig. S25. ESI-MS spectrum of 2- $\{(E)\text{-2-[5'-(dibutylamino)-2,2'-bithien-5-yl]vinyl}\}$ -1-methylpyridinium iodide

Fig. S26. ESI-MS spectrum of 2- $\{(E)\text{-2-[5'-(dibutylamino)-2,2'-bithien-5-yl]vinyl}\}$ -1-methylquinolinium iodide

Pag.29: Computational details

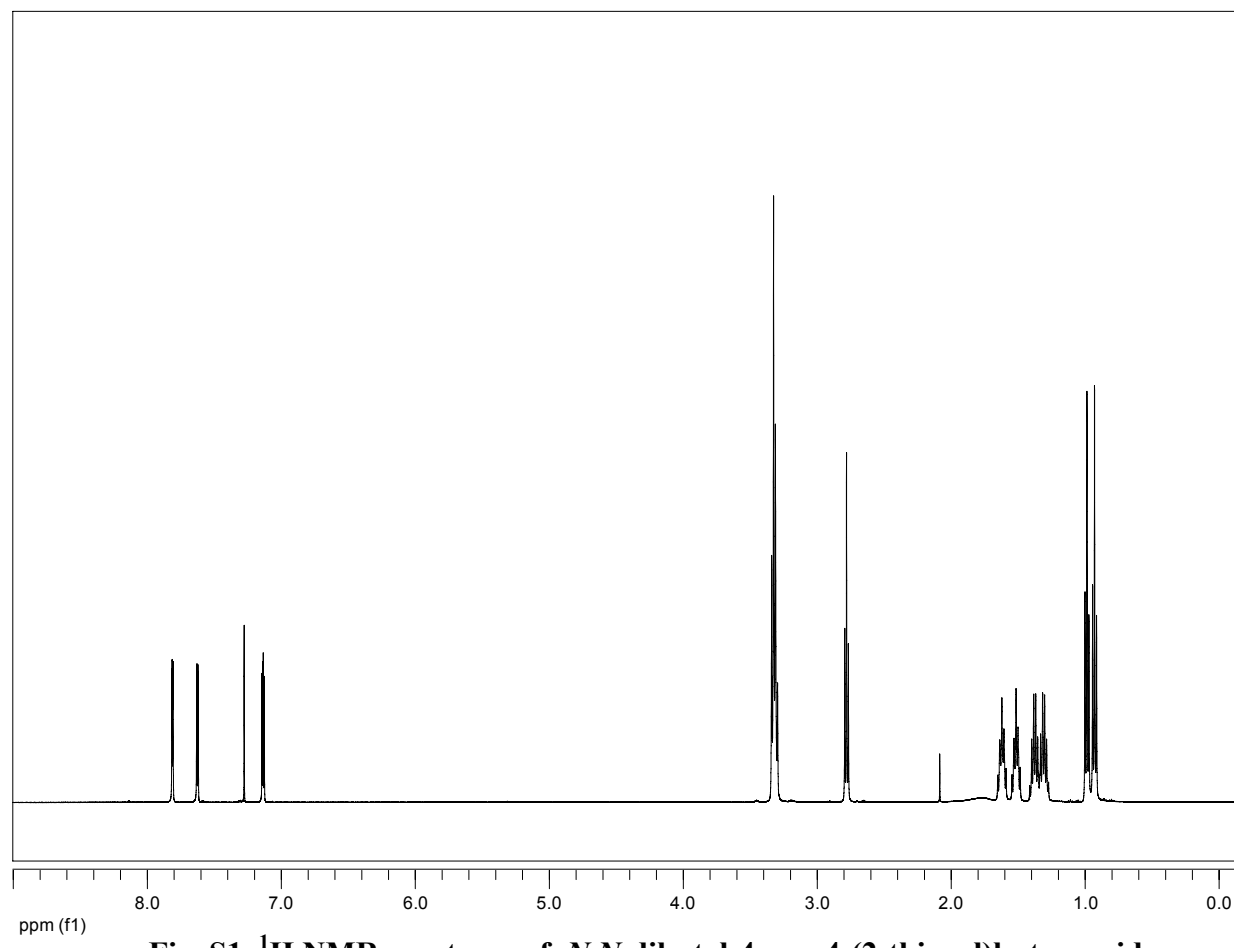


Fig. S1. ¹H NMR spectrum of *N,N*-dibutyl-4-oxo-4-(2-thienyl)butanamide

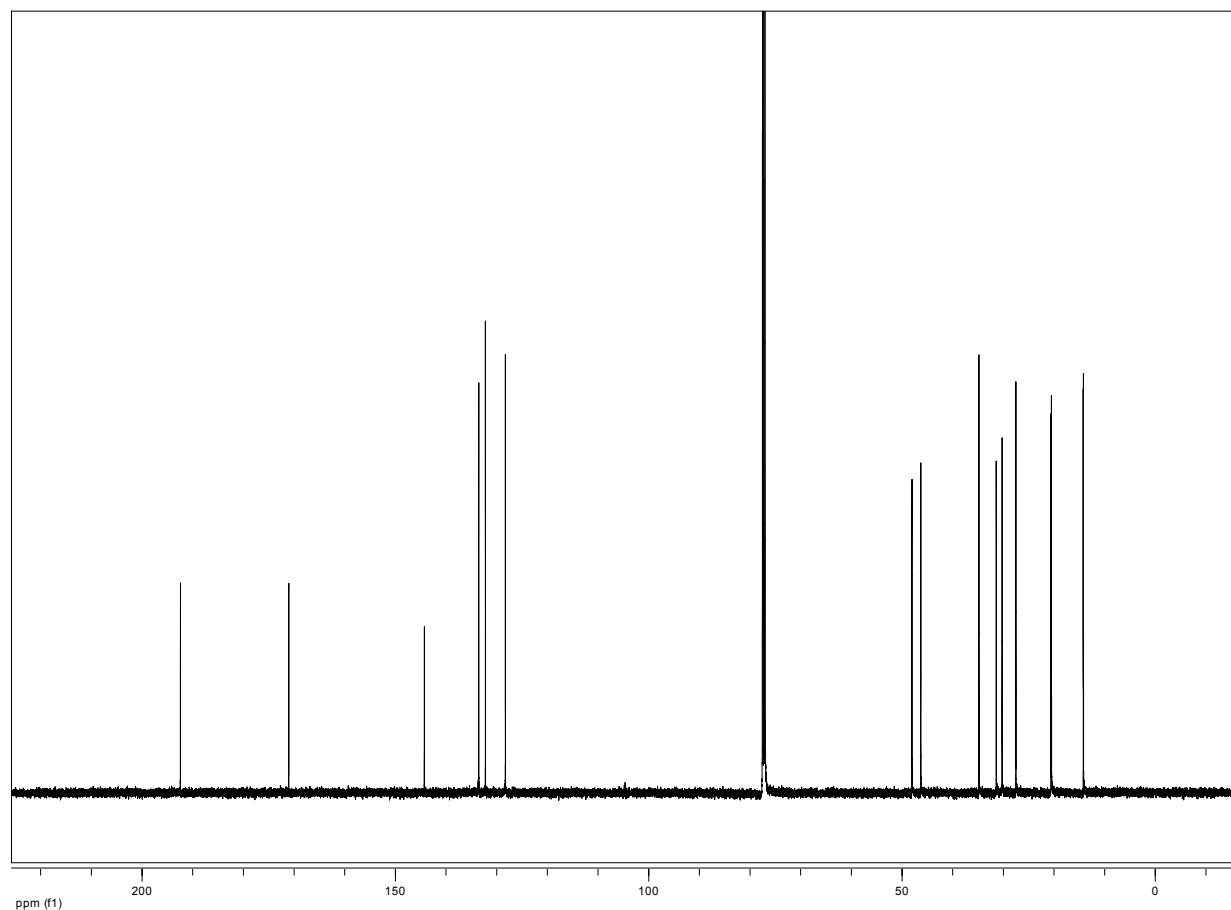


Fig. S2. ¹³C NMR spectrum of *N,N*-dibutyl-4-oxo-4-(2-thienyl)butanamide

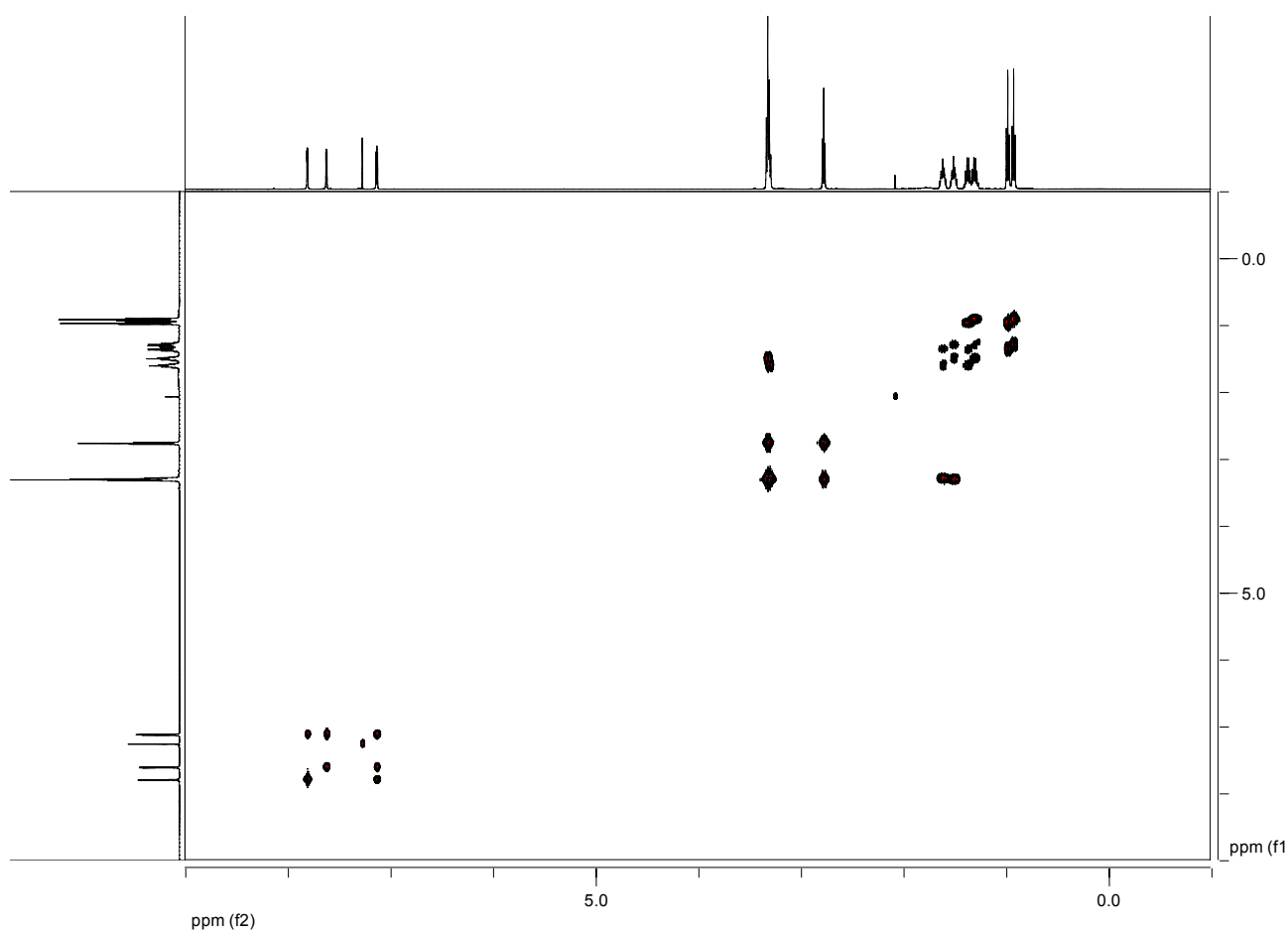


Fig. S3. ^1H - ^1H gCOSY NMR spectrum of *N,N*-dibutyl-4-oxo-4-(2-thienyl)butanamide

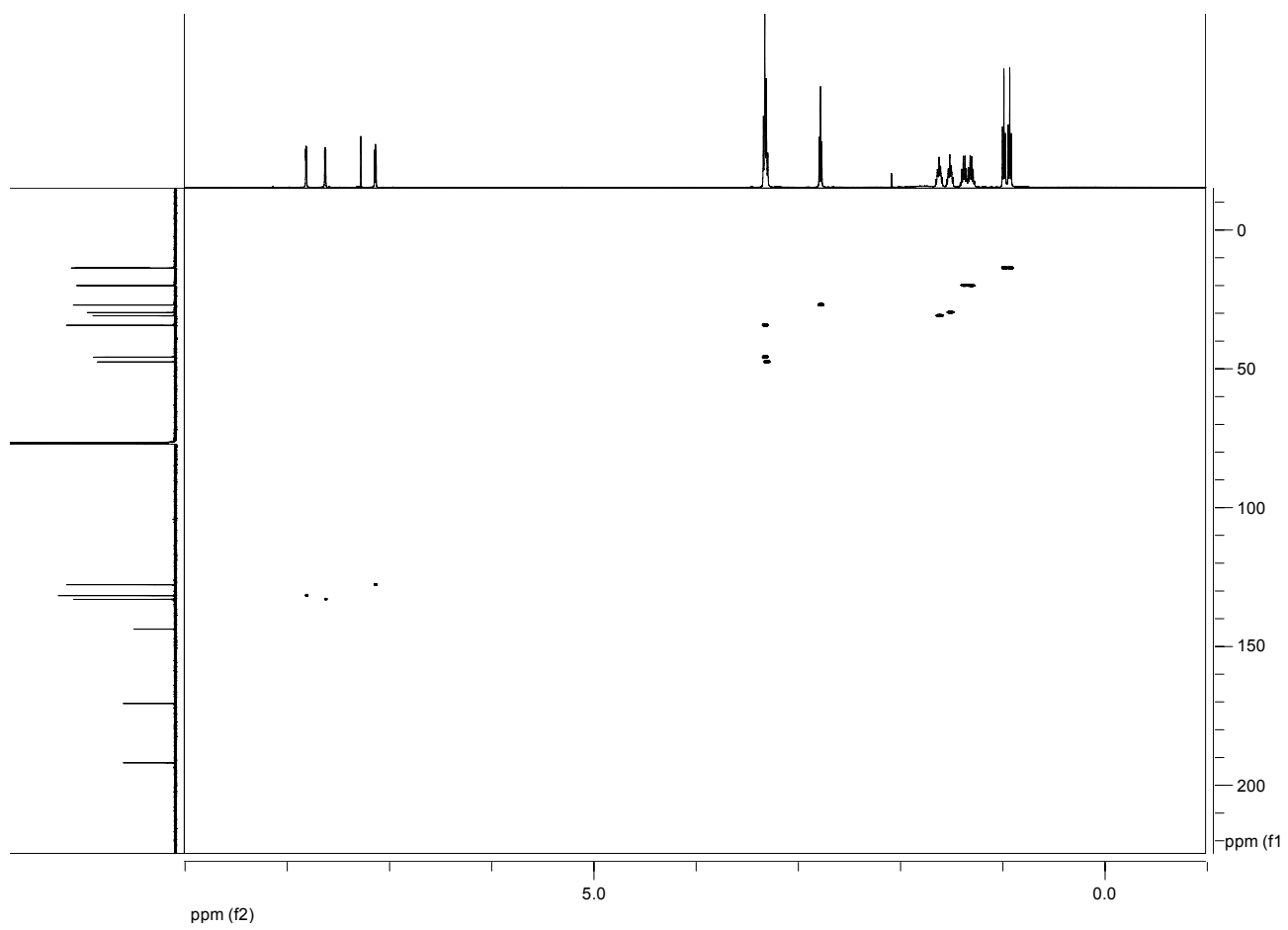


Fig. S4. ¹H-¹³C gHSQCAD NMR spectrum of *N,N*-dibutyl-4-oxo-4-(2-thienyl)butanamide

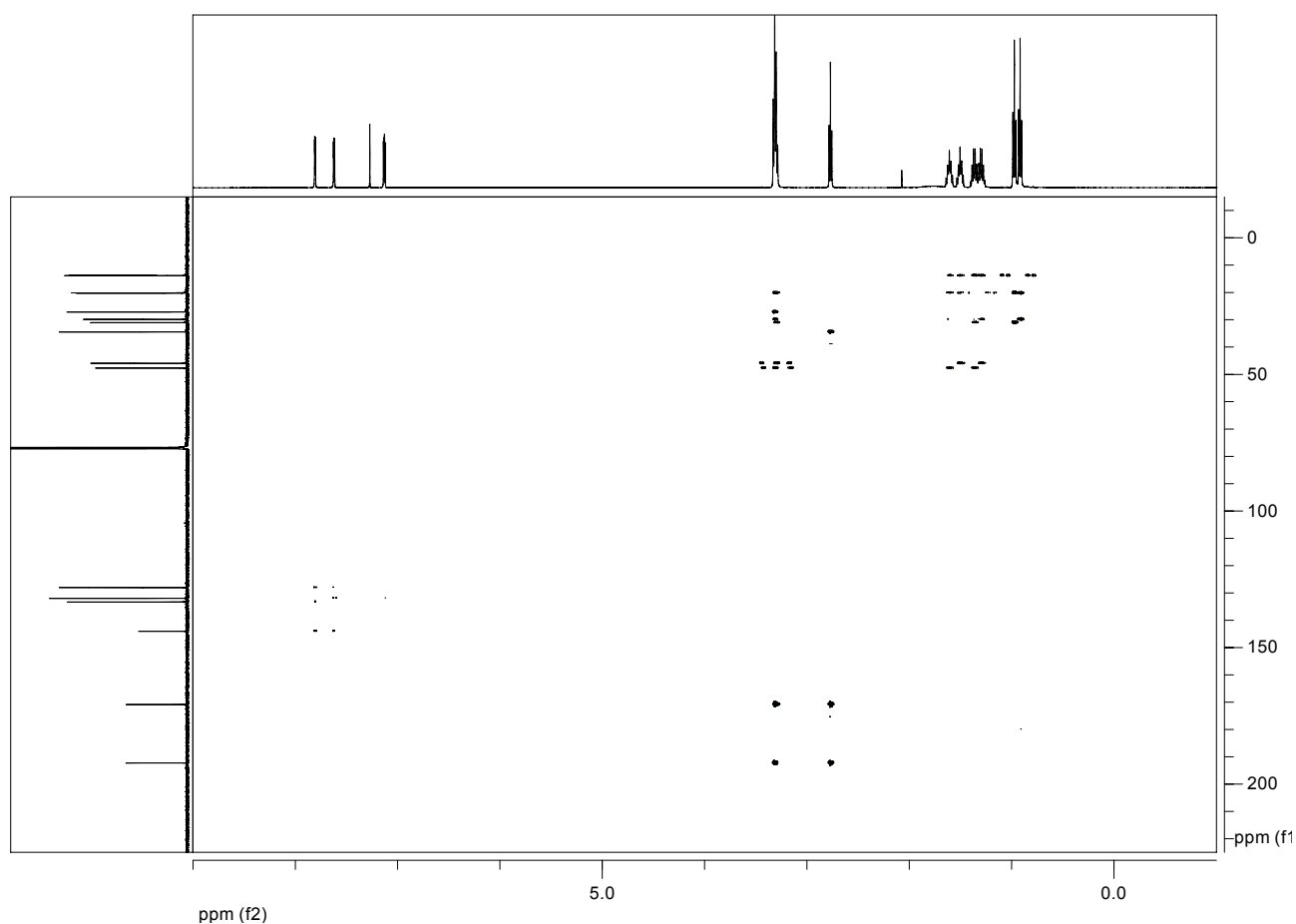


Fig. S5. ¹H-¹³C gHMBCAD NMR spectrum of *N,N*-dibutyl-4-oxo-4-(2-thienyl)butanamide

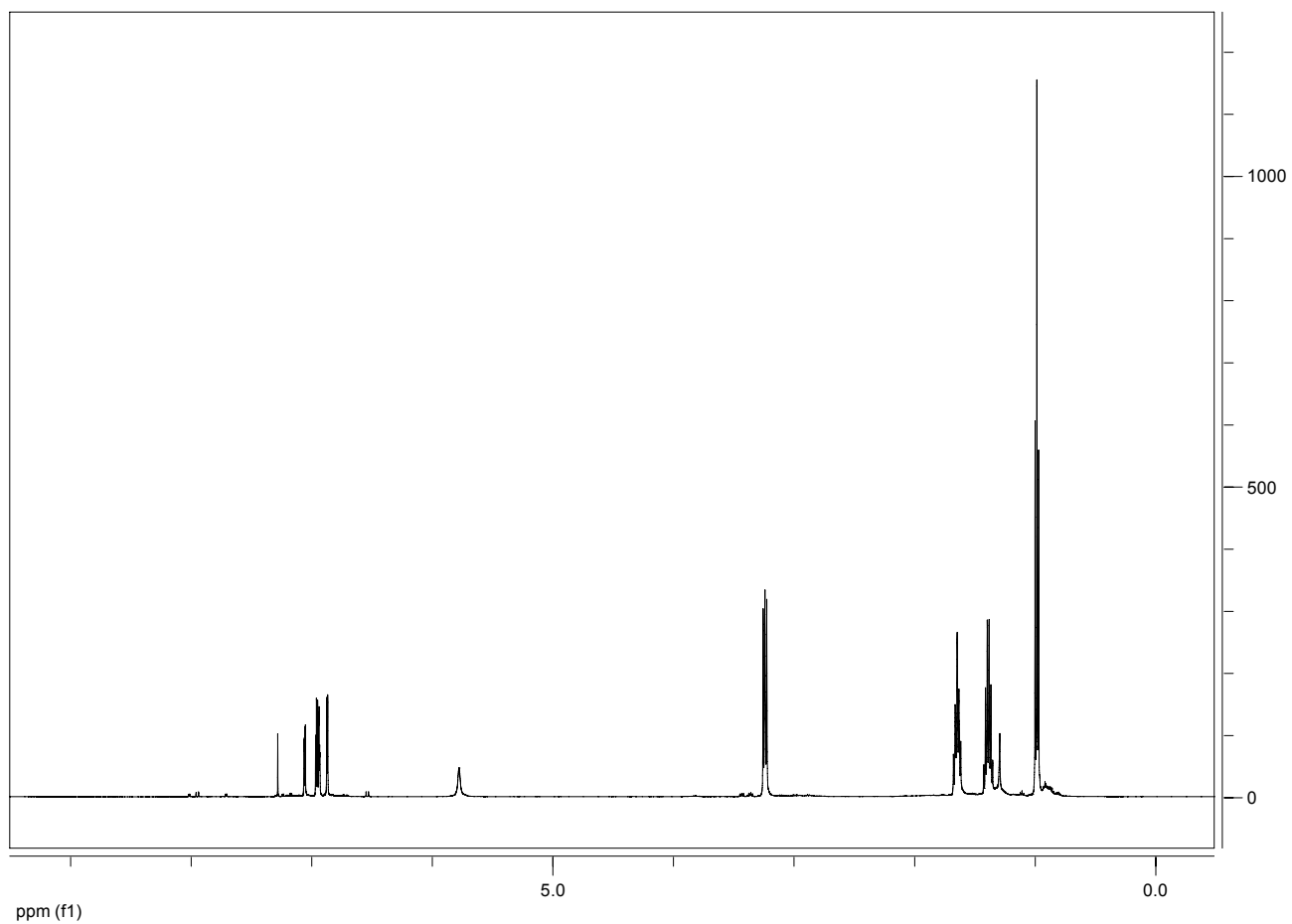


Fig. S6. ^1H NMR spectrum of *N,N*-dibutyl-2,2'-bithiophen-5-amine

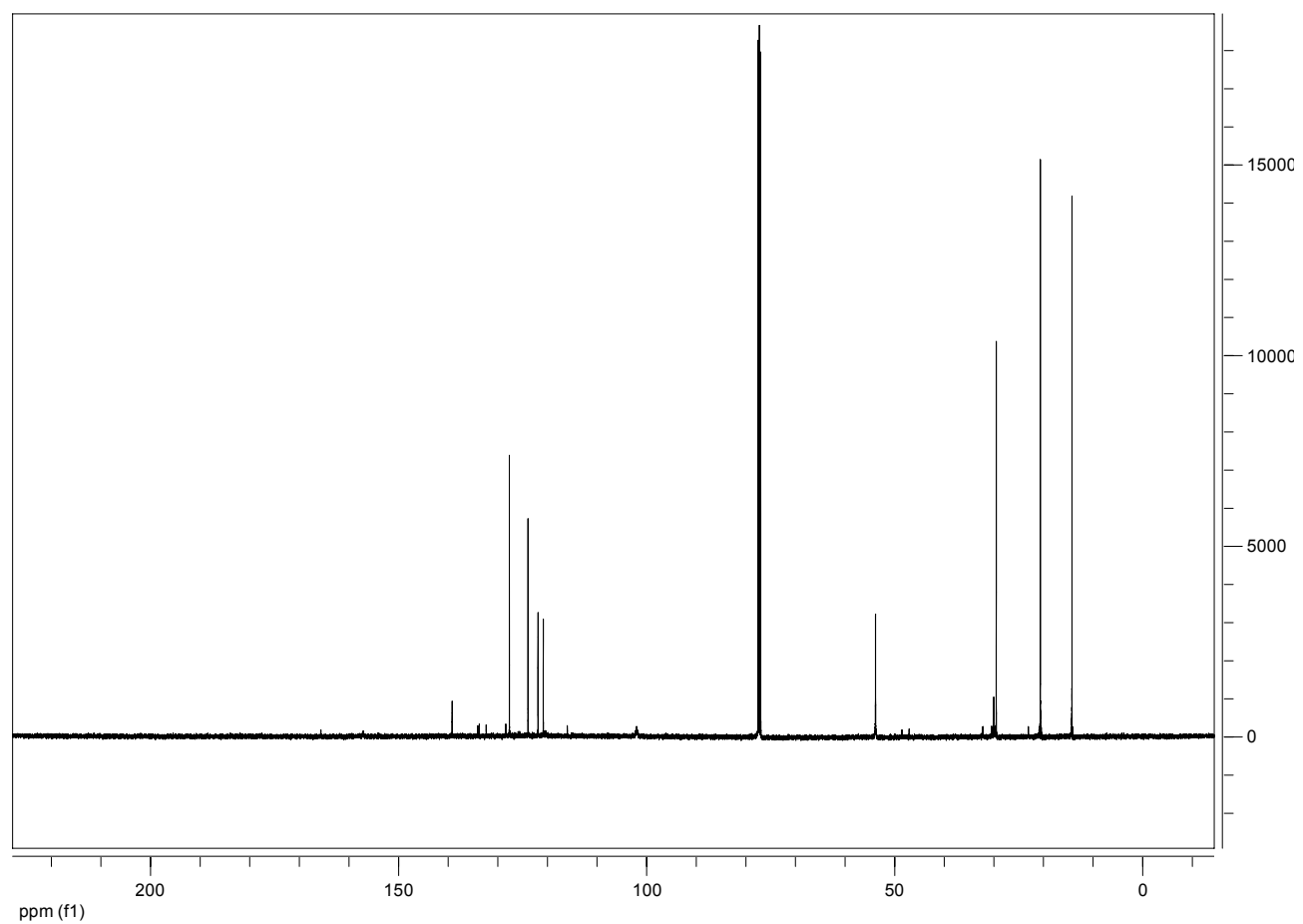


Fig. S7. ^{13}C NMR spectrum of *N,N*-dibutyl-2,2'-bithiophen-5-amine

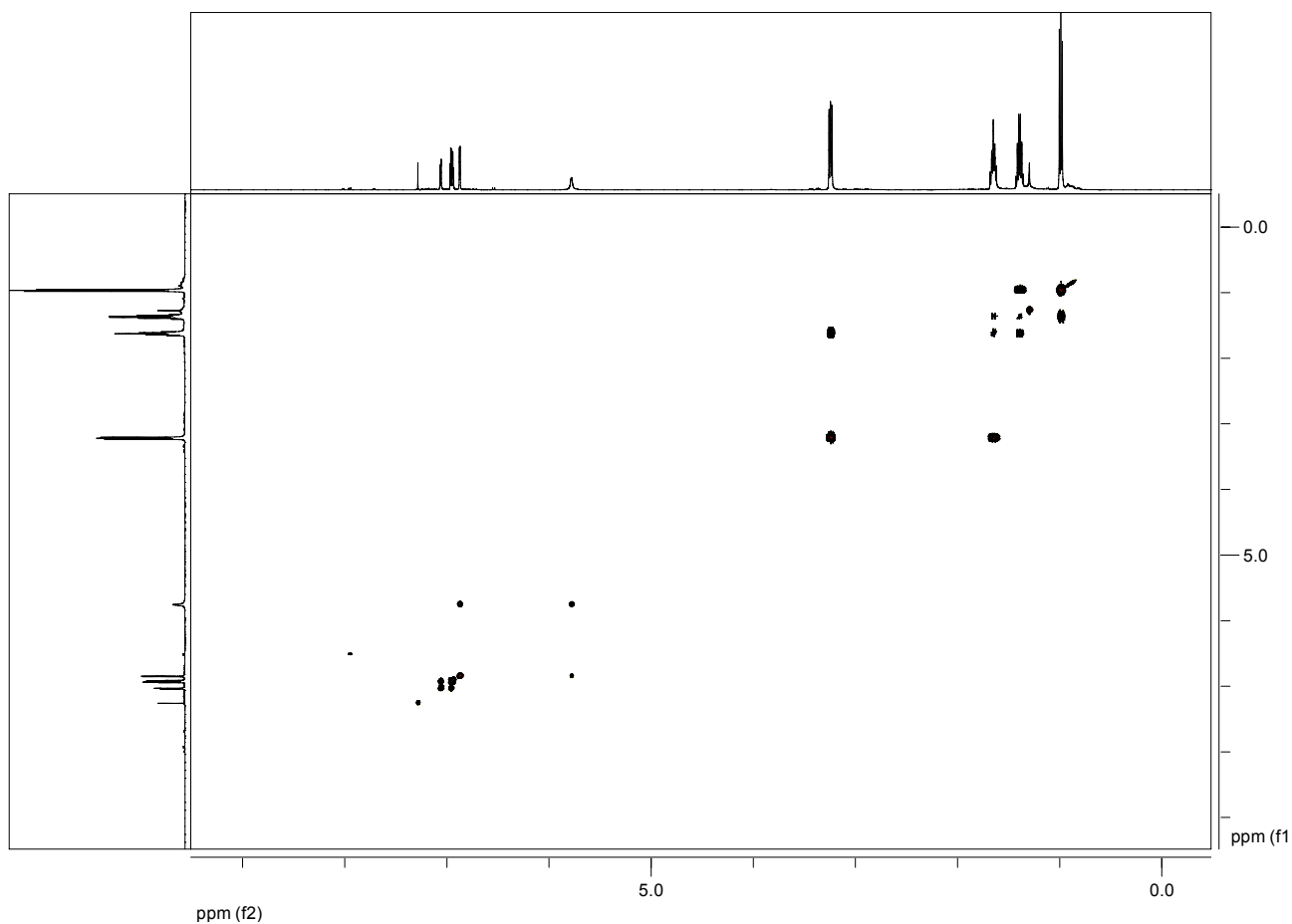


Fig. S8. ^1H - ^1H gCOSY NMR spectrum of *N,N*-dibutyl-2,2'-bithiophen-5-amine

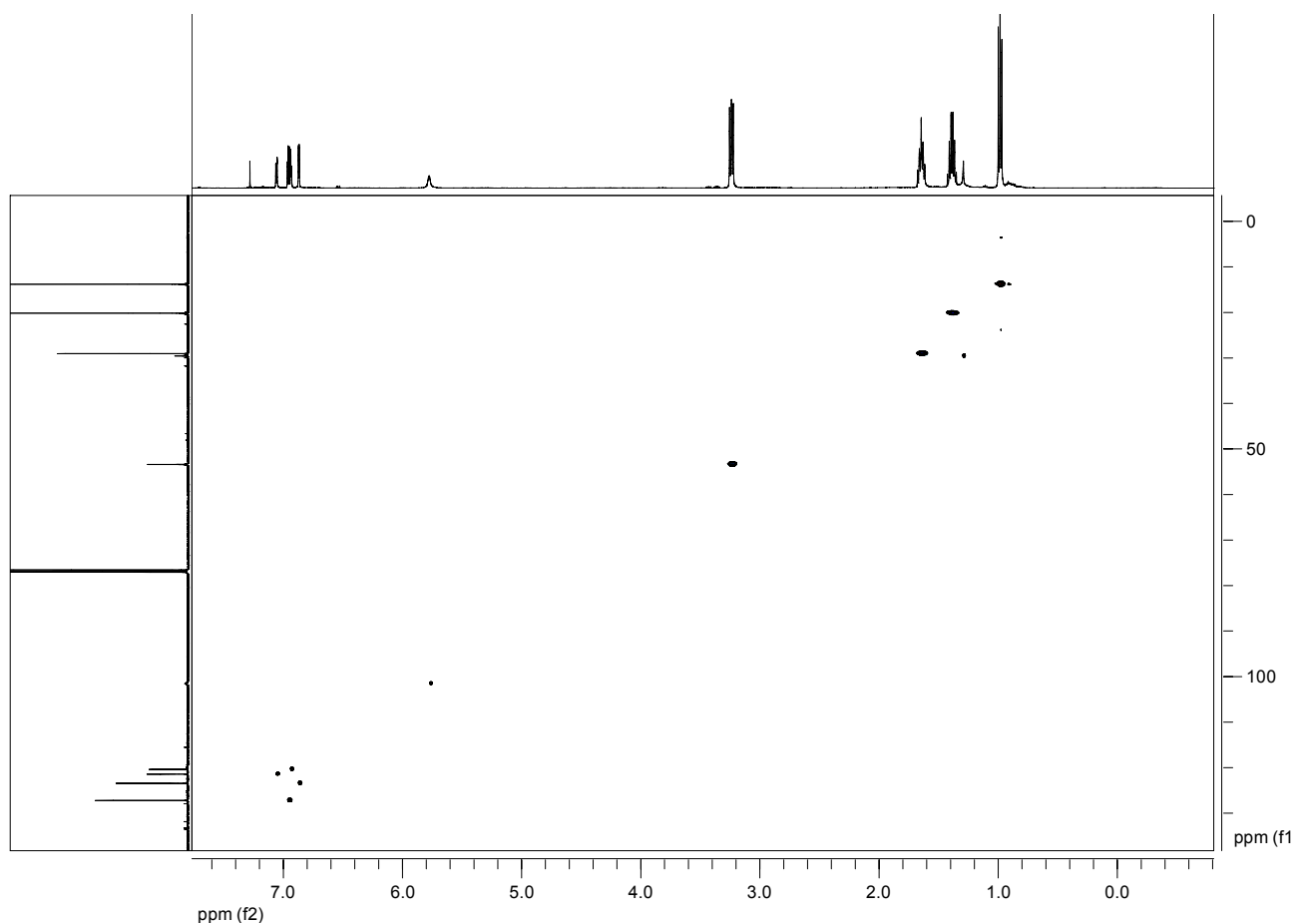


Fig. S9. ^1H - ^{13}C gHSQCAD NMR spectrum of *N,N*-dibutyl-2,2'-bithiophen-5-amine

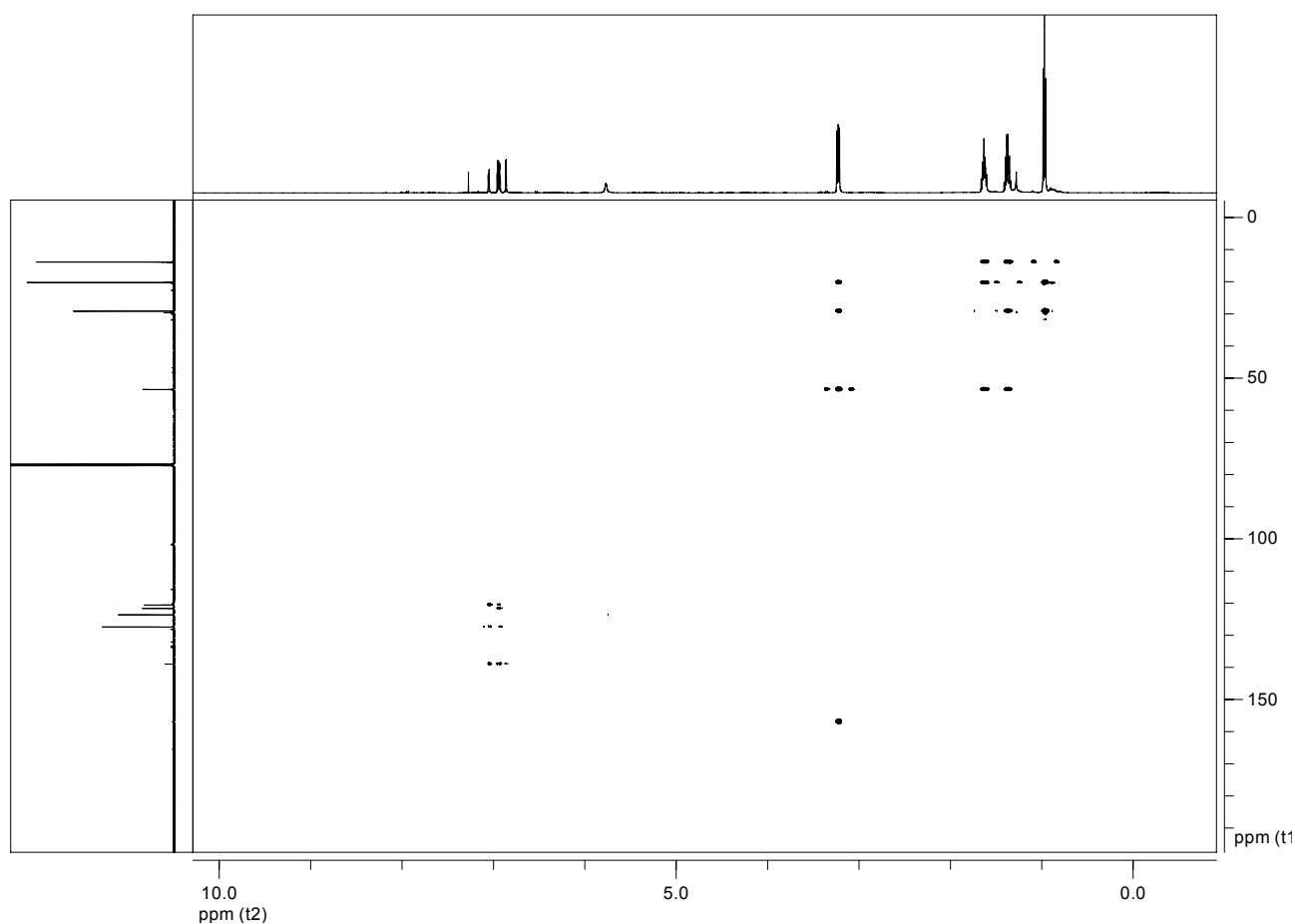


Fig. S10. ^1H - ^{13}C gHMBCAD NMR spectrum of *N,N*-dibutyl-2,2'-bithiophen-5-amine

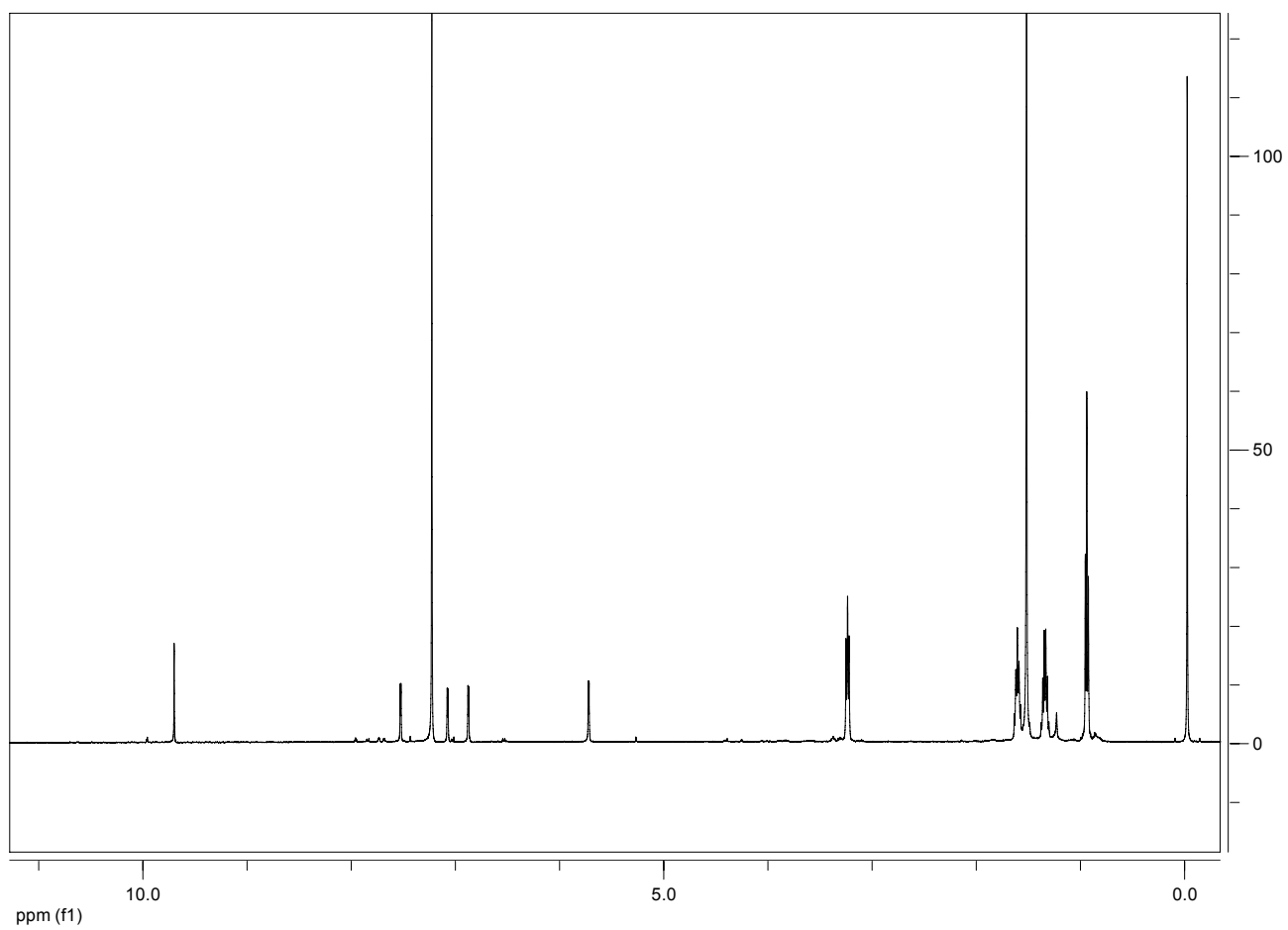


Fig. S11. ^1H NMR spectrum of 5'-(dibutylamino)-2,2'-bithiophene-5-carbaldehyde

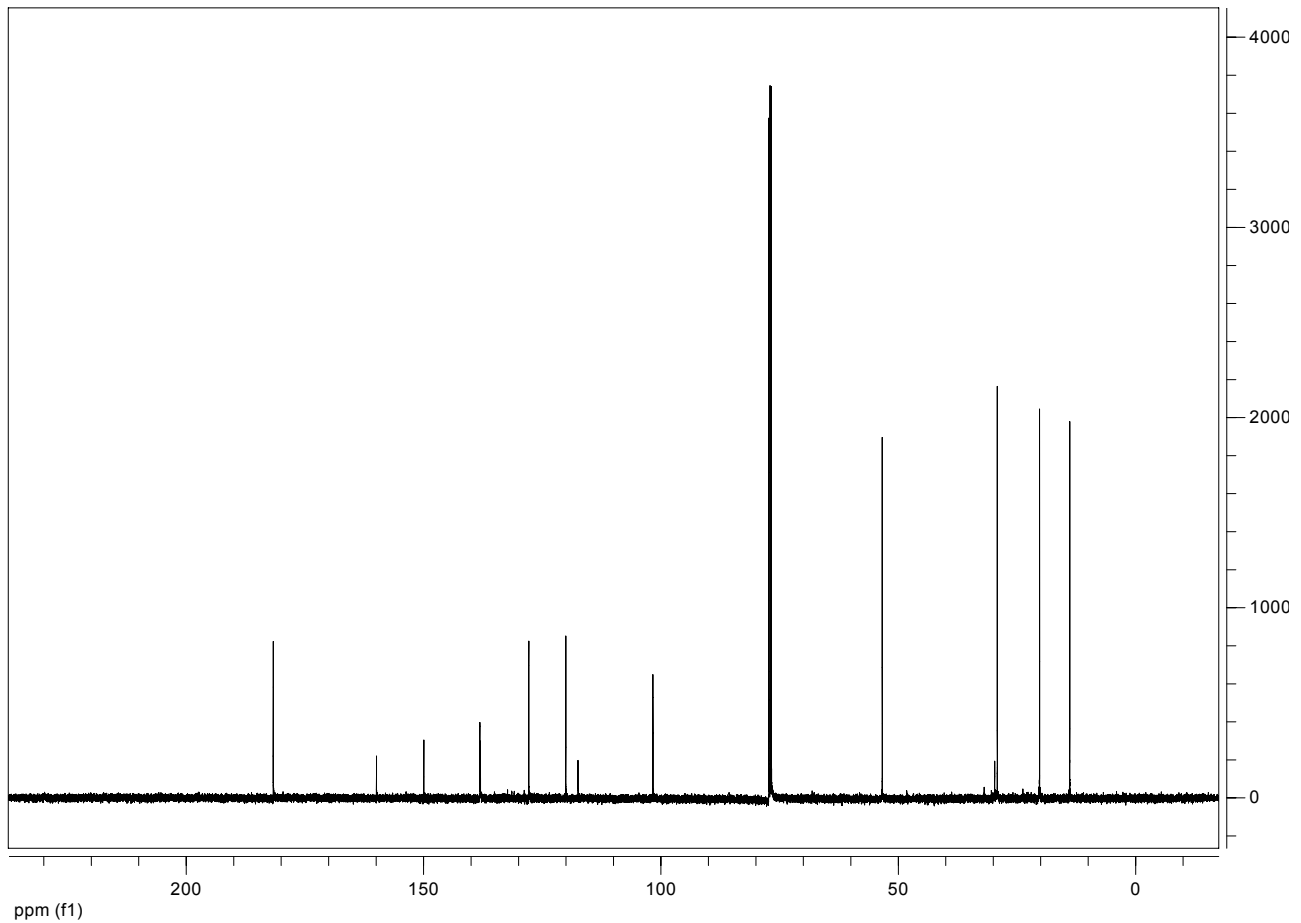


Fig. S12. ^{13}C NMR spectrum of 5'-(dibutylamino)-2,2'-bithiophene-5-carbaldehyde

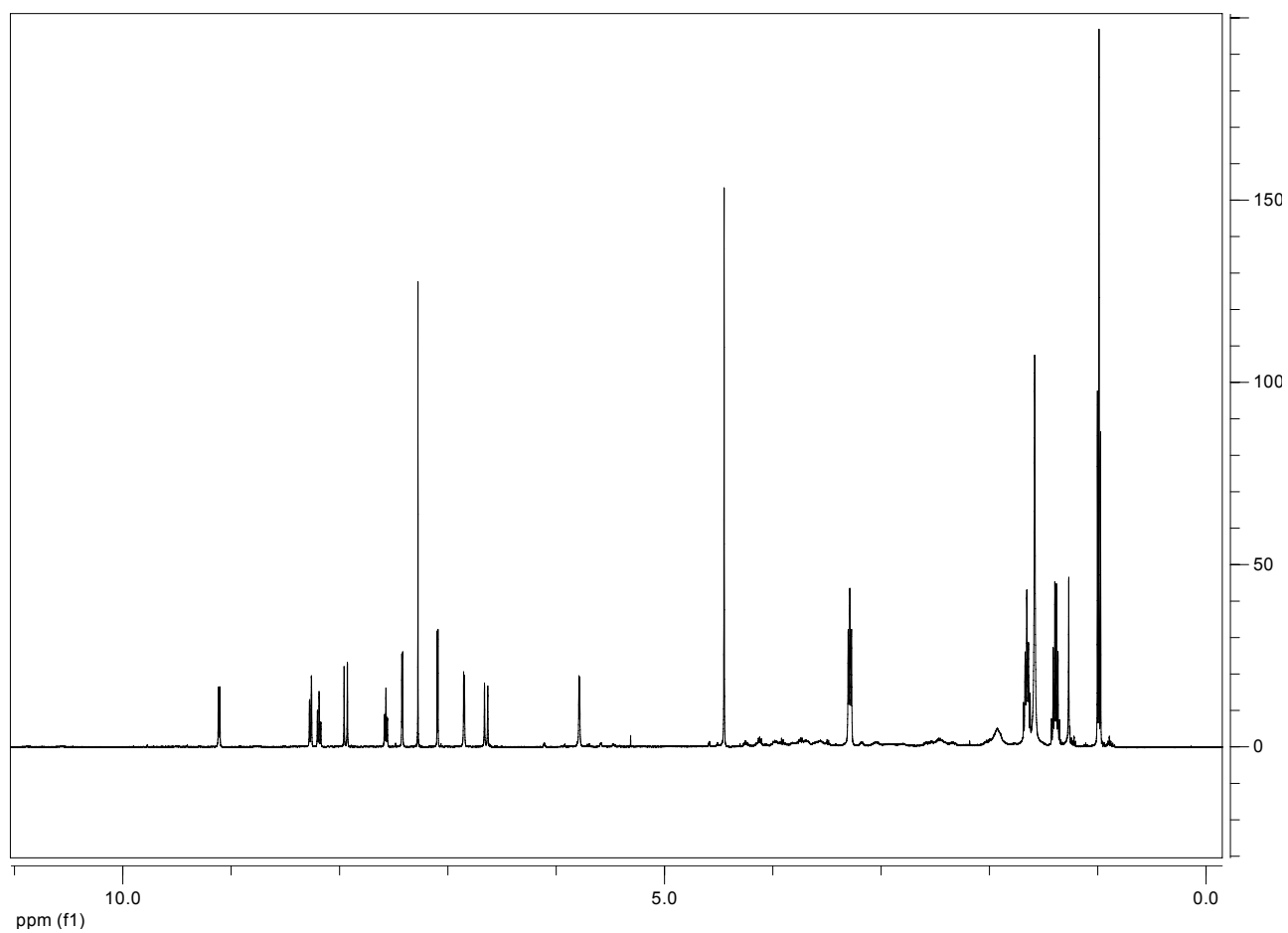


Fig. S13. ¹H NMR spectrum of 2-{(E)-2-[5'-(dibutylamino)-2,2'-bithien-5-yl]vinyl}-1-methylpyridinium iodide

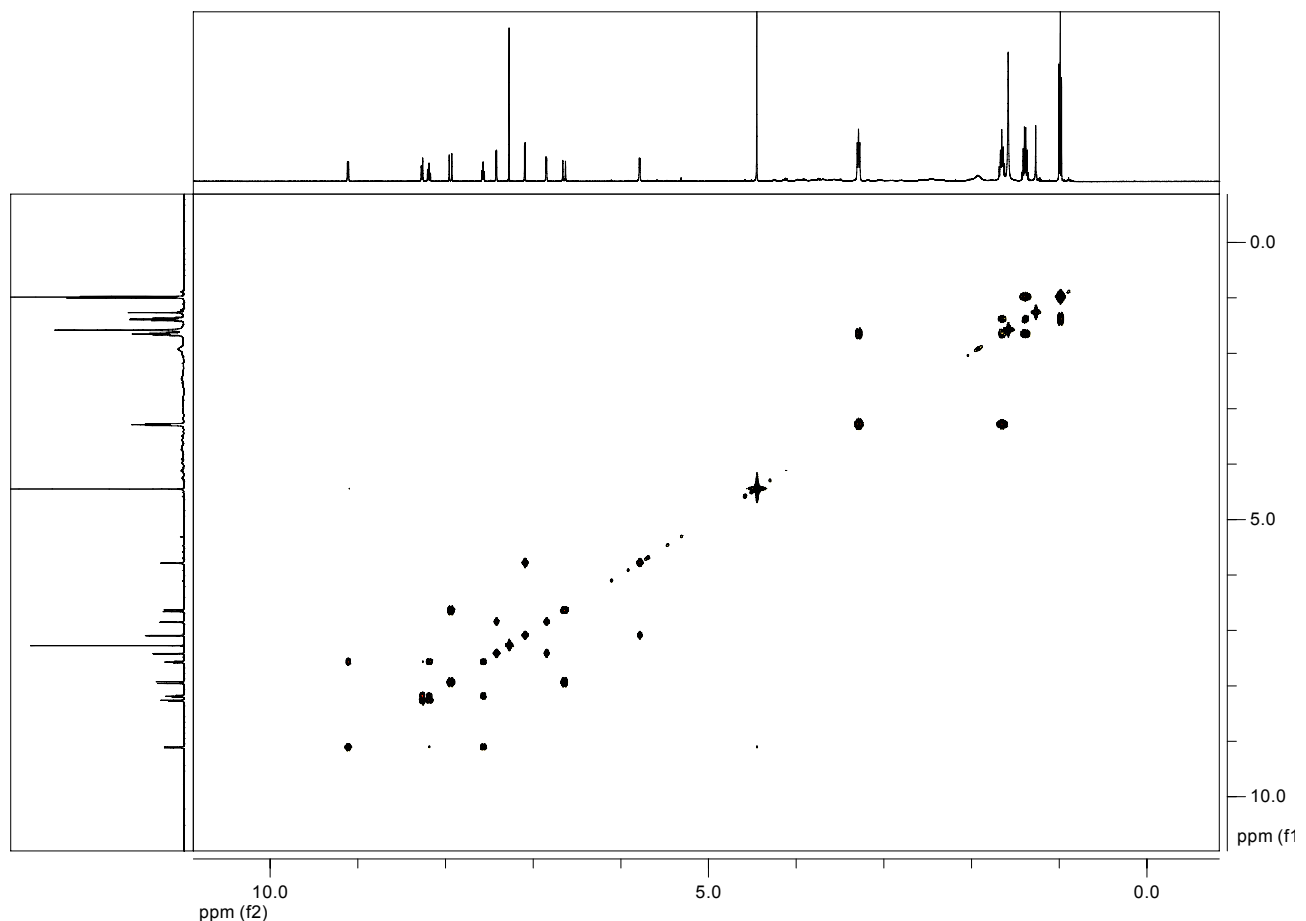


Fig. S14. ¹H-¹H gCOSY NMR spectrum of 2-{(E)-2-[5'-(dibutylamino)-2,2'-bithien-5-yl]vinyl}-1-methylpyridinium iodide

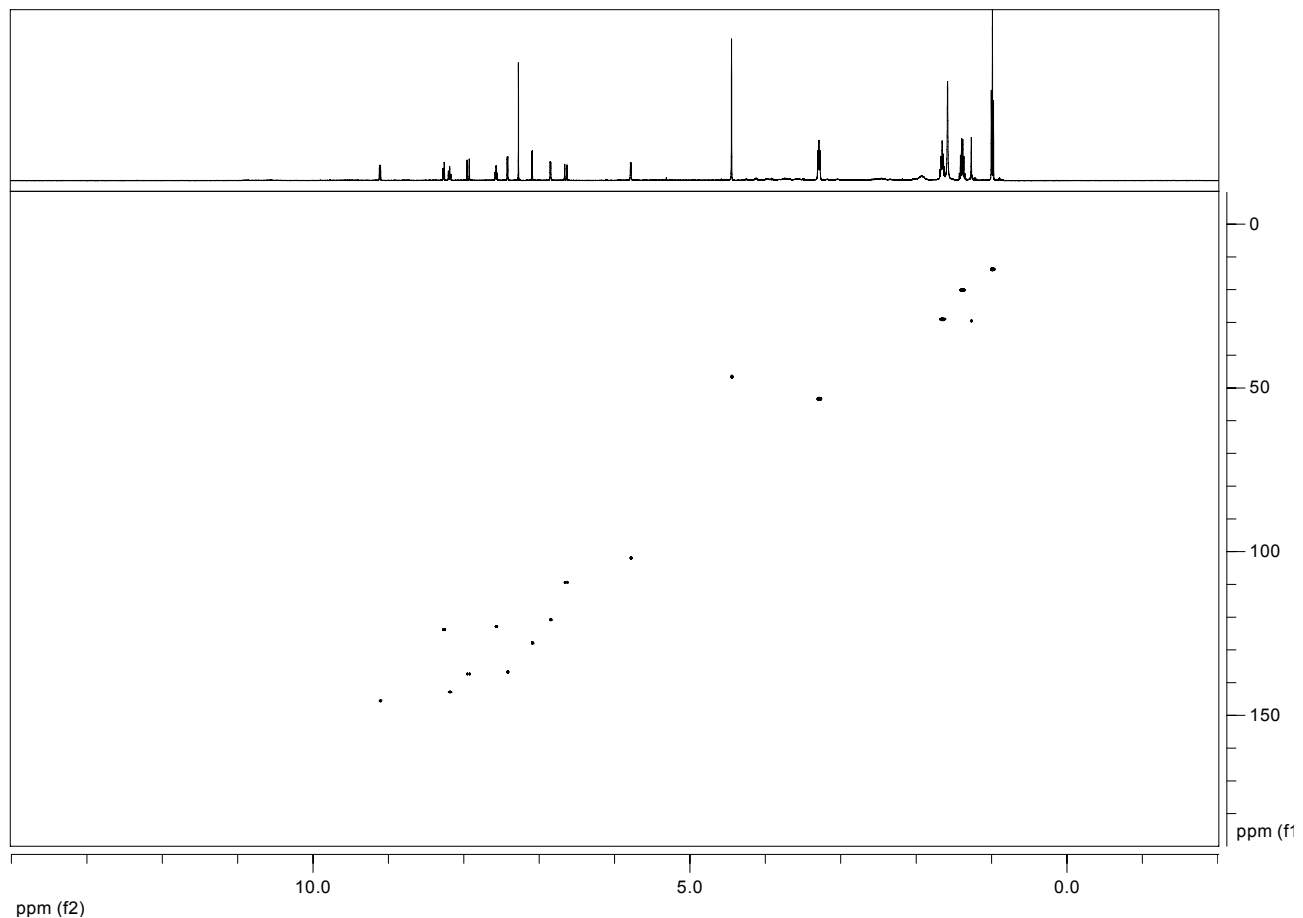


Fig. S15. ¹H-¹³C gHSQCAD NMR spectrum of 2-{(E)-2-[5'-(dibutylamino)-2,2'-bithien-5-yl]vinyl}-1-methylpyridinium iodide

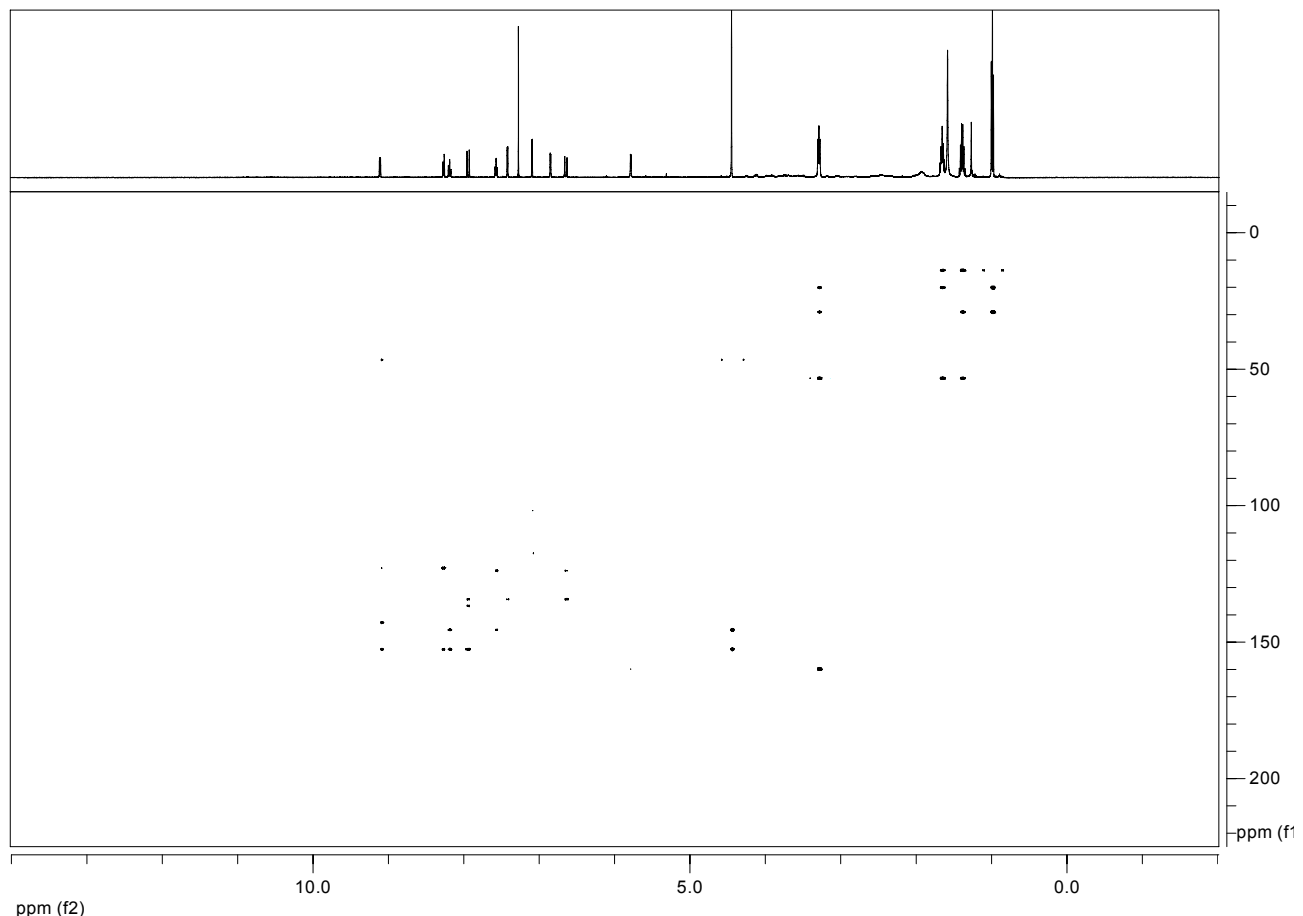


Fig. S16. ¹H-¹³C gHMBCAD NMR spectrum of 2-{(E)-2-[5'-(dibutylamino)-2,2'-bithien-5-yl]vinyl}-1-methylpyridinium iodide

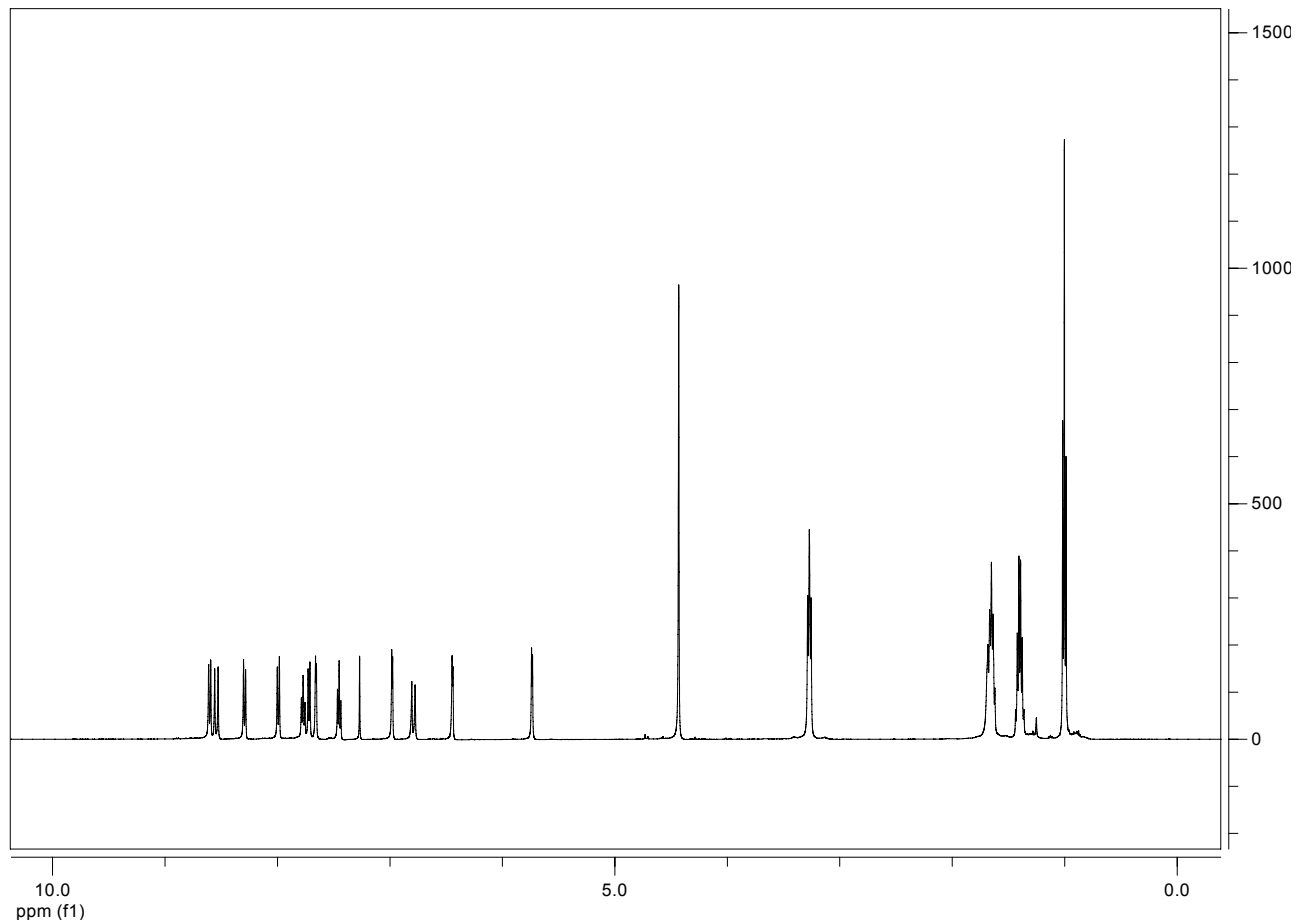


Fig. S17. ¹H NMR spectrum of 2-{(E)-2-[5'-(dibutylamino)-2,2'-bithien-5-yl]vinyl}-1-methylquinolinium iodide

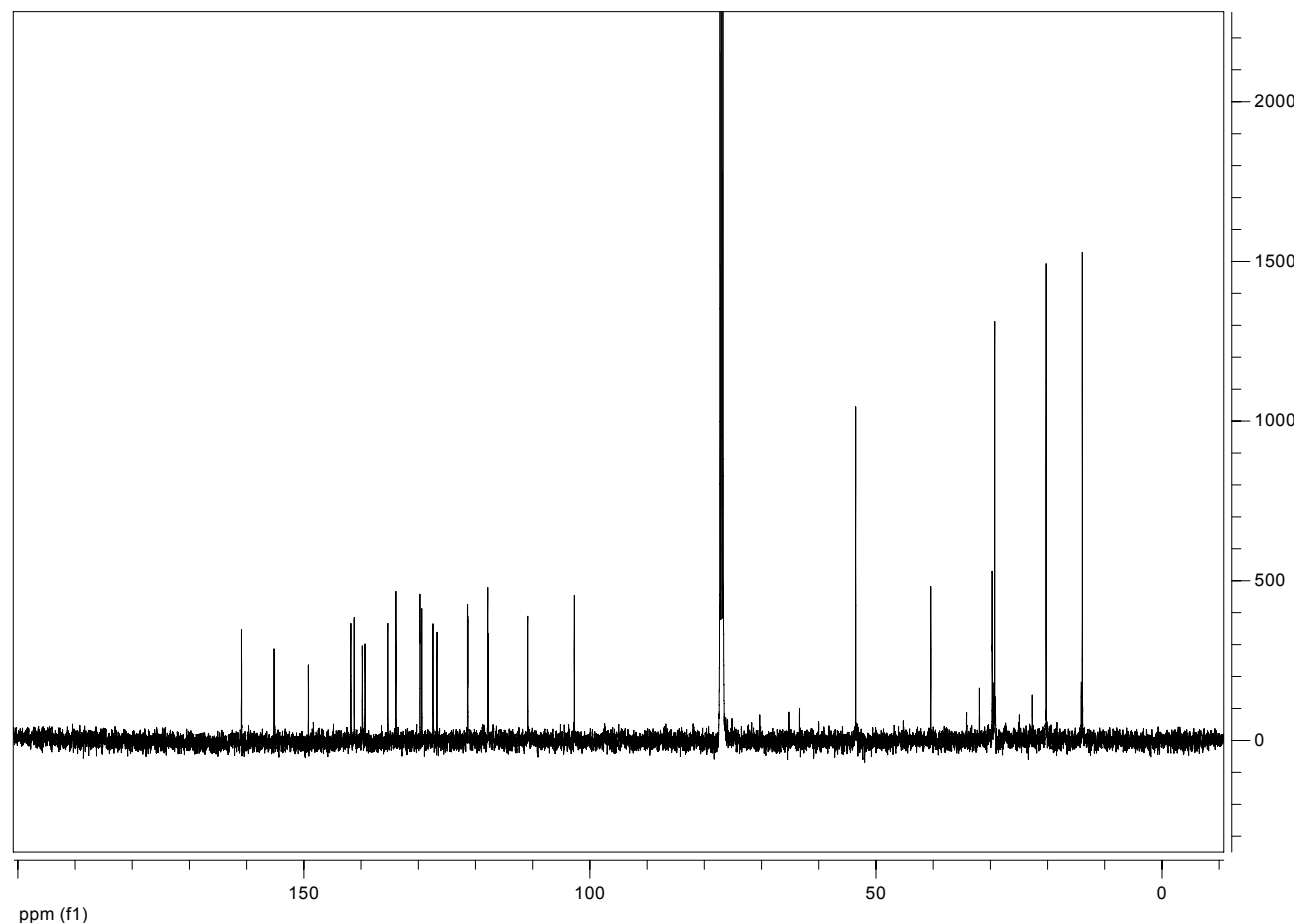


Fig. S18. ^{13}C NMR spectrum of 2-{(E)-2-[5'-(dibutylamino)-2,2'-bithien-5-yl]vinyl}-1-methylquinolinium iodide

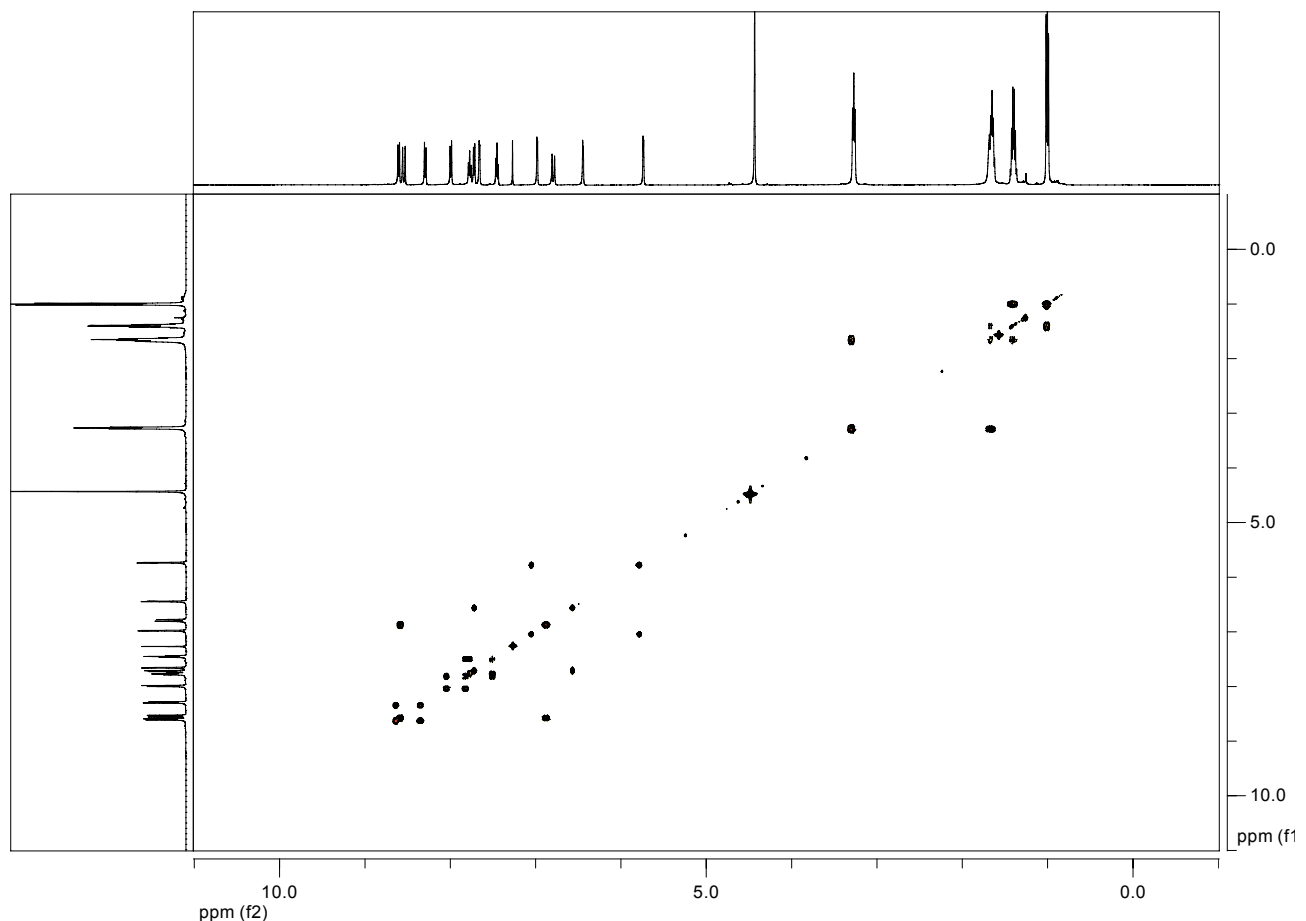


Fig. S19. ¹H-¹H gCOSY NMR spectrum of 2-{(E)-2-[5'-(dibutylamino)-2,2'-bithien-5-yl]vinyl}-1-methylquinolinium iodide

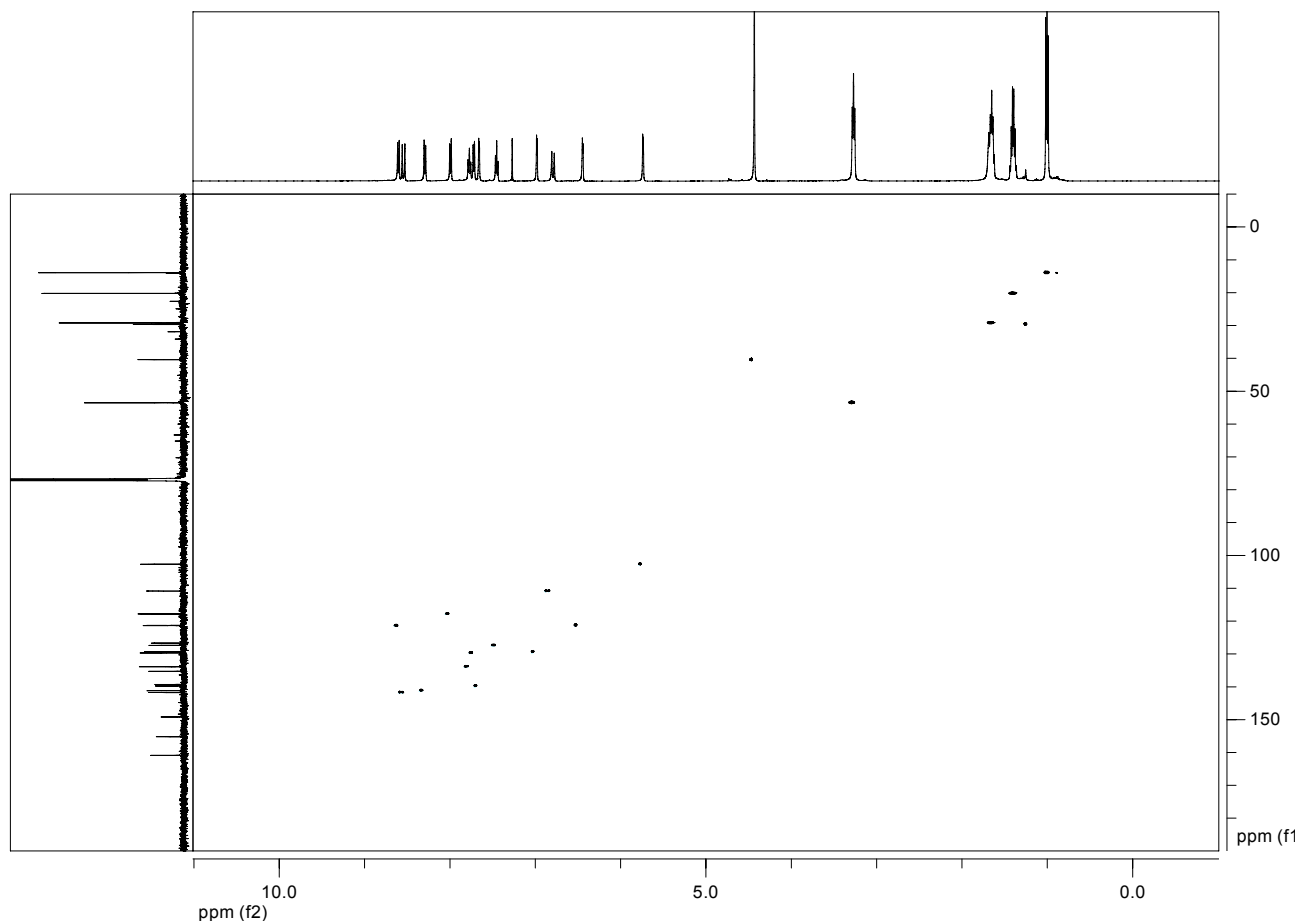


Fig. S20. ¹H-¹³C gHSQCAD NMR spectrum of 2-{(E)-2-[5'-(dibutylamino)-2,2'-bithien-5-yl]vinyl}-1-methylquinolinium iodide

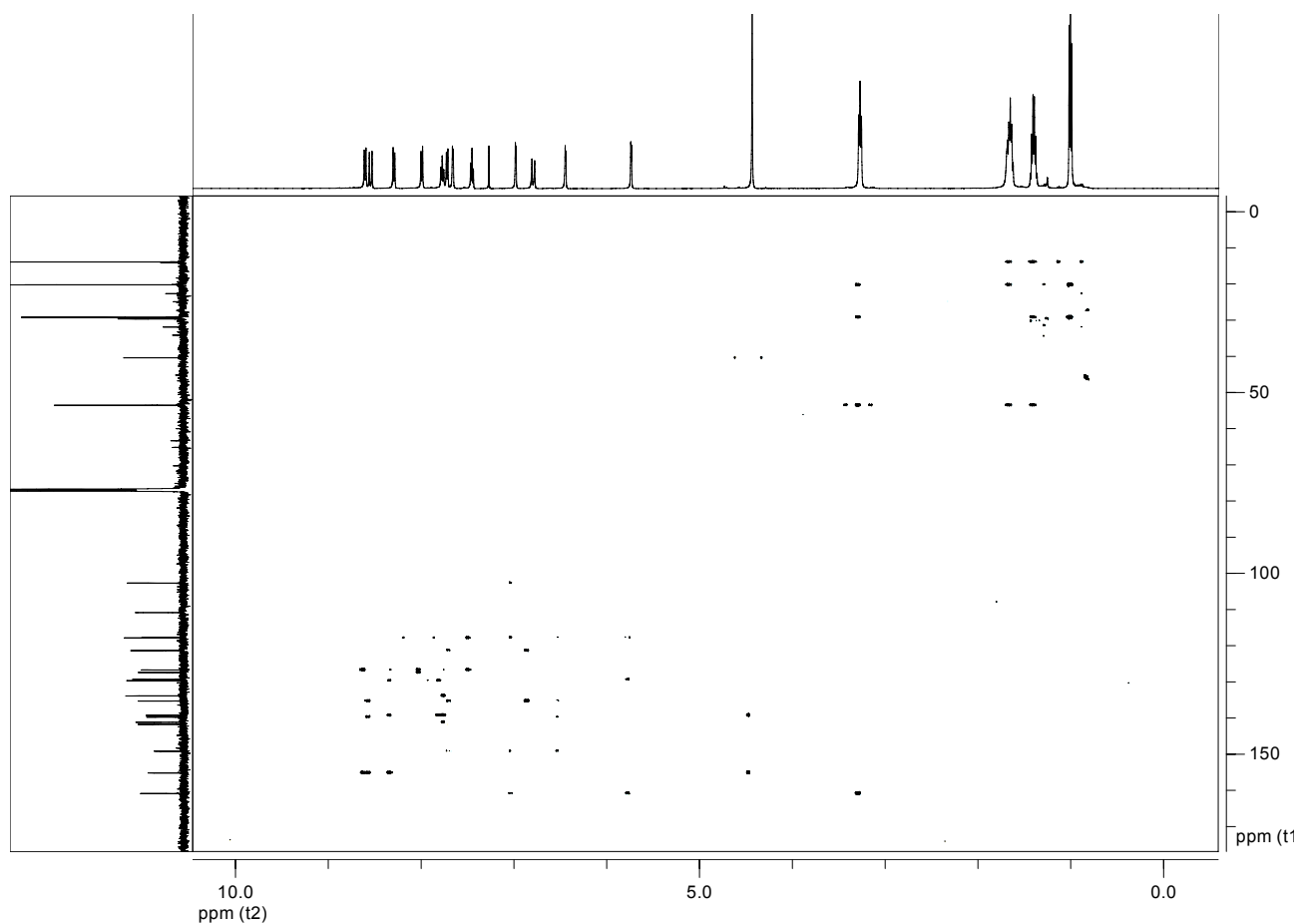


Fig. S21. ¹H-¹³C gHMBCAD NMR spectrum of 2-{(E)-2-[5'-(dibutylamino)-2,2'-bithien-5-yl]vinyl}-1-methylquinolinium iodide

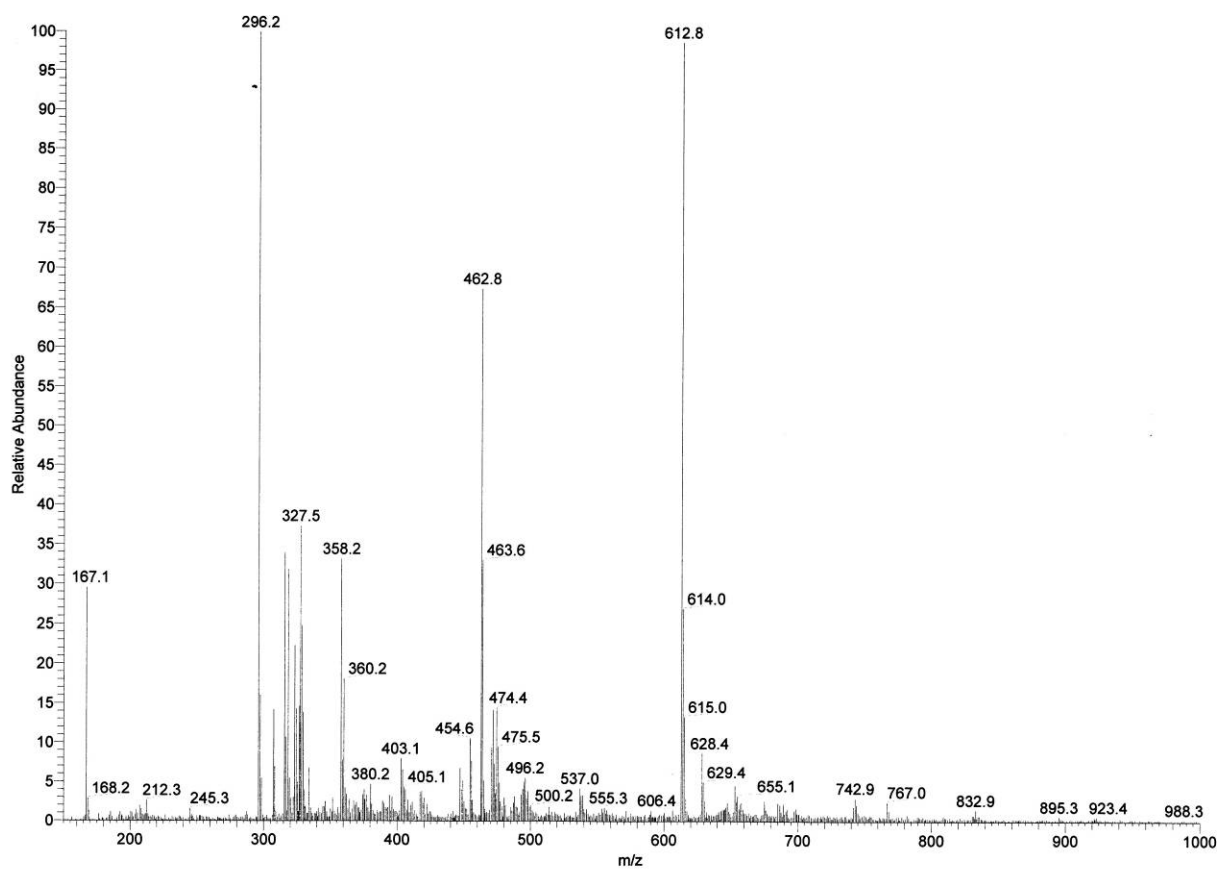


Fig. S22. ESI-MS spectrum of *N,N*-dibutyl-4-oxo-4-(2-thienyl)butanamide

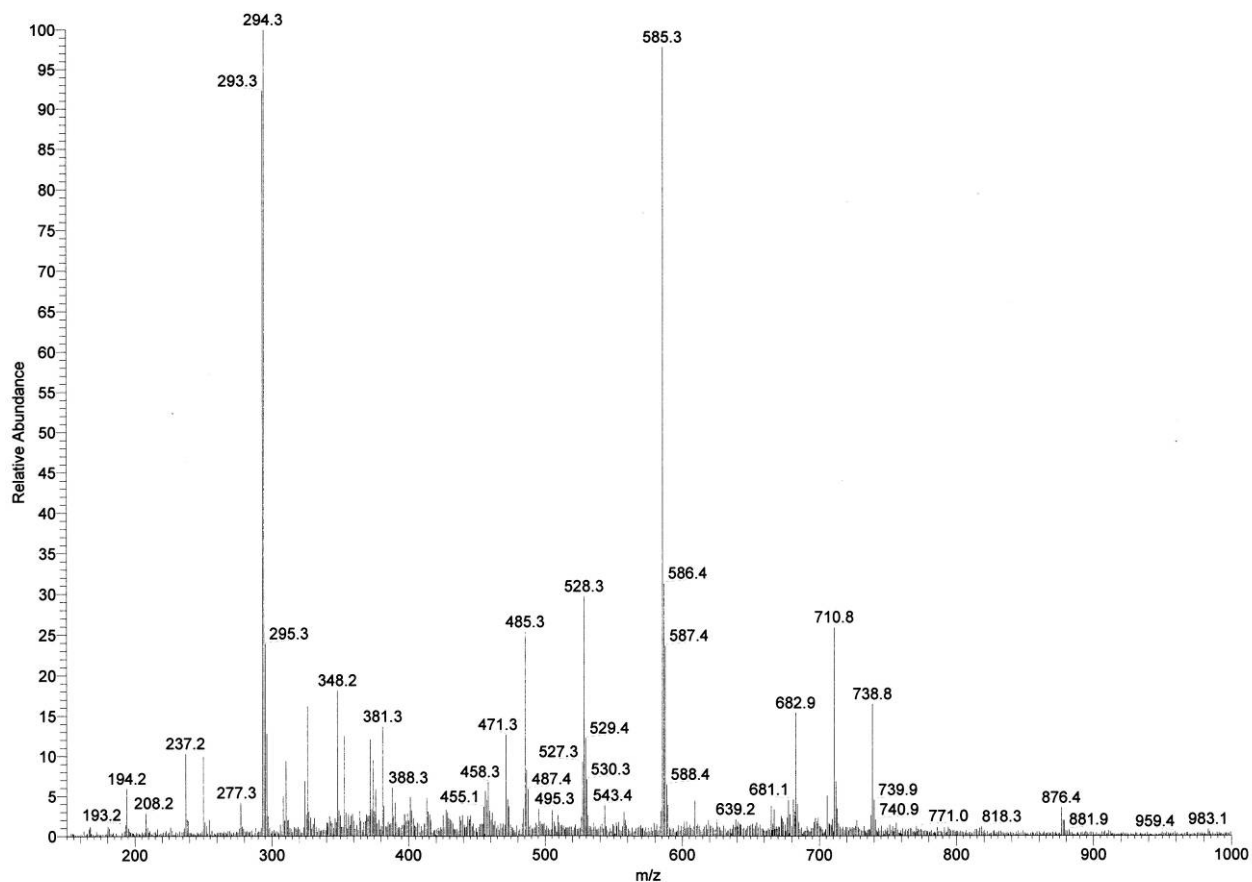


Fig. S23. ESI-MS spectrum of *N,N*-dibutyl-2,2'-bithiophen-5-amine

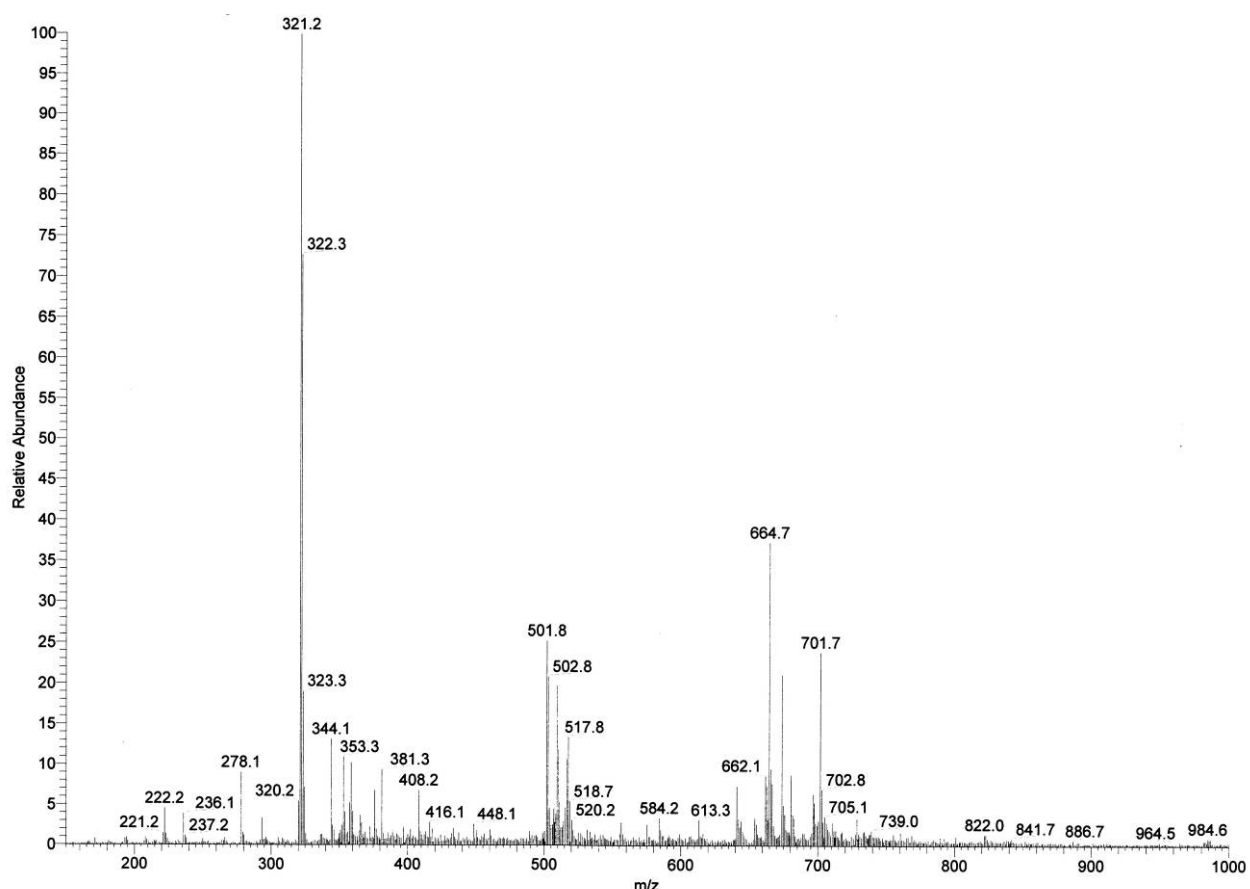


Fig. S24. ESI-MS spectrum of 5'-(dibutylamino)-2,2'-bithiophene-5-carbaldehyde

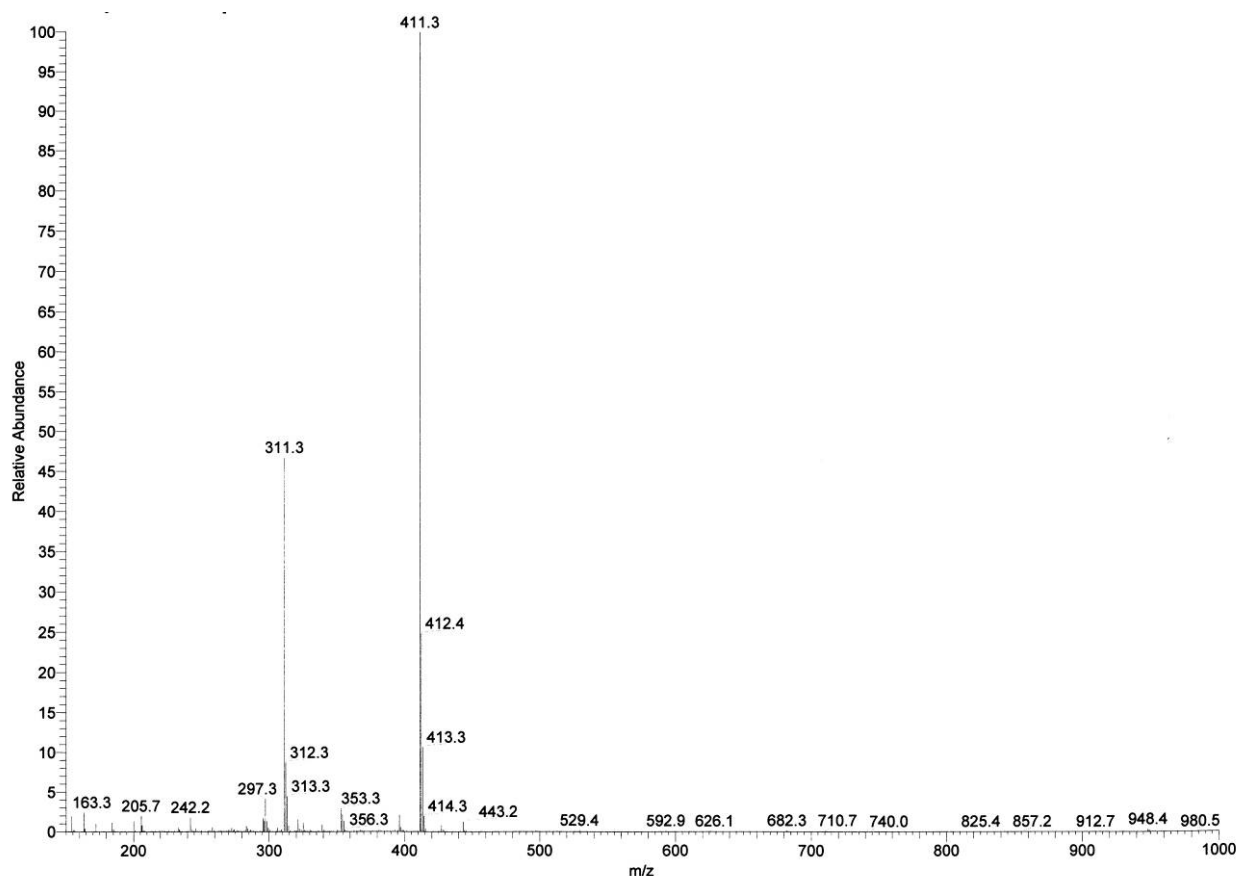


Fig. S25. ESI-MS spectrum of 2-{(E)-2-[5'-(dibutylamino)-2,2'-bithien-5-yl]vinyl}-1-methylpyridinium iodide

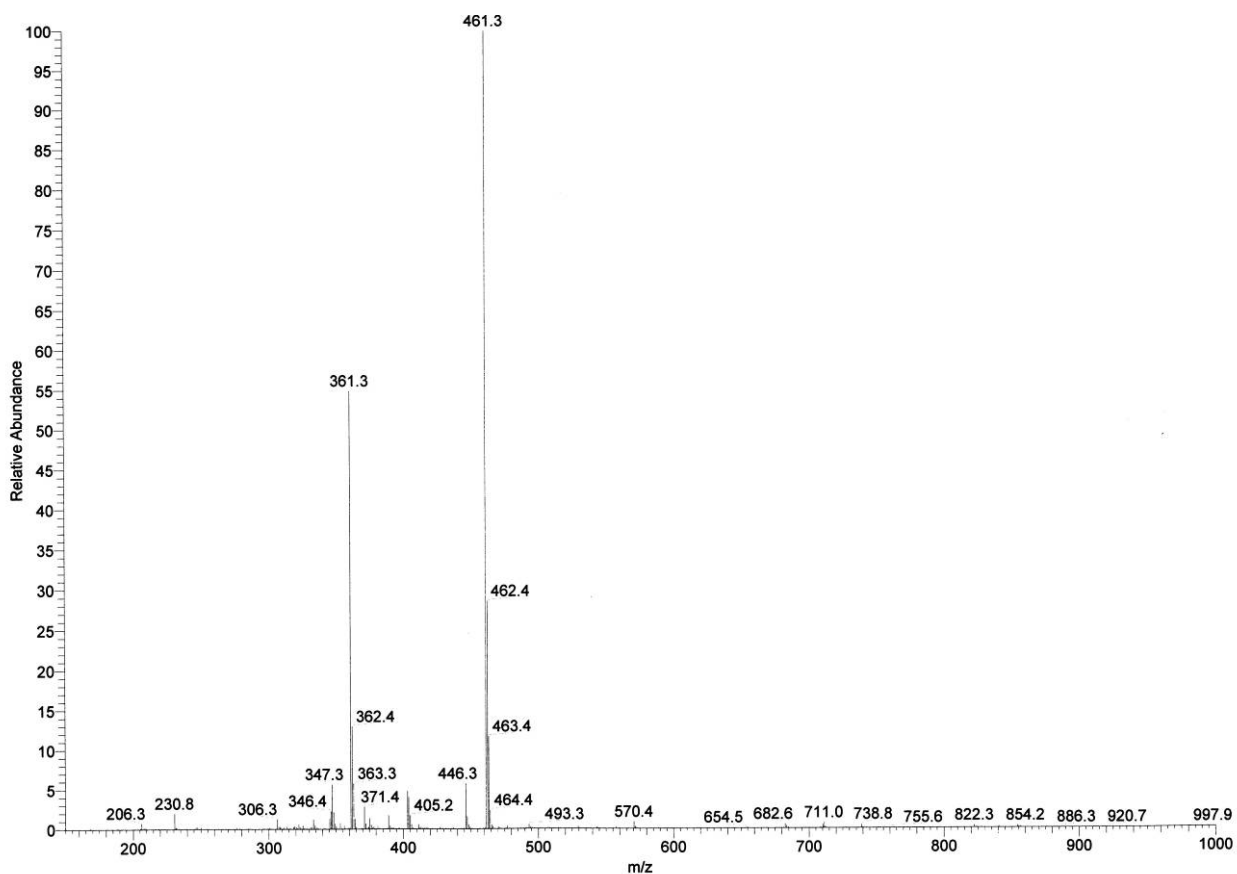


Fig. S26. ESI-MS spectrum of 2-{(E)-2-[5'-(dibutylamino)-2,2'-bithien-5-yl]vinyl}-1-methylquinolinium iodide

Computational details

All calculations in this work were carried out using the GAUSSIAN 03 package.ⁱ The geometrical structures for the model compounds were obtained at the density functional theory (DFT) B3LYP/6-311+G(d,p) level; after the minimization process, the vibrational spectra have been evaluated to check that no imaginary frequencies are present. The static first hyperpolarizabilities (β_0) are evaluated by the coupled perturbed Hartree Fock (CPHF) approach at the Hartree-Fock level with 6-311+G(d,p) basis set for all the atoms. Solvation effects were taken into account using the Polarizable Continuum Model.

The dipole moment (μ_0) and polarizability (α_0) are defined as follow:

$$\mu_0 = (\mu_x^2 + \mu_y^2 + \mu_z^2)^{1/2}$$

$$\alpha_0 = \frac{1}{3}(\alpha_{xx} + \alpha_{yy} + \alpha_{zz})$$

The static first hyperpolarizability is noted as

$$\beta_0 = (\beta_x^2 + \beta_y^2 + \beta_z^2)^{1/2}$$

where

$$\beta_i = \frac{3}{5}(\beta_{iii} + \beta_{ijj} + \beta_{ikk}) \quad i,j,k=x,y,z$$

TABLE S1: Calculated Dipole Moment (μ_0 , D), Polarizability (α_0 , au) and First Hyperpolarizability (β_0 , au, 10^{-30} esu).

	μ_0	α_0	β_0 (au)	β_0 (10^{-30} esu)
1c	15.6	373	15768	136
1d	13.0	509	49772	430

B3LYP/6-311+G(d,p) geometries (cartesian coordinates) and energies (atomic unit)

Compound **1c**

Center Number	Atomic Number	Atomic Type	Coordinates (Angstroms)		
			X	Y	Z
1	6	0	5.776403	1.088365	0.037869
2	6	0	6.486260	-0.084351	-0.047675
3	6	0	5.769902	-1.291398	-0.125751
4	6	0	4.390427	-1.267454	-0.116073
5	6	0	3.669349	-0.054430	-0.021952
6	7	0	4.412692	1.108188	0.052953
7	1	0	6.294879	-2.238475	-0.200543
8	1	0	6.261700	2.054616	0.099446
9	1	0	7.569228	-0.055614	-0.056272
10	1	0	3.840107	-2.196109	-0.193421
11	6	0	2.232562	0.025487	-0.009857
12	6	0	1.394826	-1.058144	0.030823
13	1	0	1.784110	1.010321	-0.033873
14	1	0	1.808597	-2.063113	0.077144
15	6	0	3.745972	2.424075	0.158857
16	1	0	3.146944	2.614008	-0.734663
17	1	0	3.114756	2.451141	1.049502
18	1	0	4.510665	3.194219	0.242335
19	6	0	-0.026934	-1.033226	0.032154
20	6	0	-0.859321	-2.149704	0.089035
21	16	0	-0.991846	0.436556	-0.037259
22	6	0	-2.228442	-1.840591	0.077524
23	1	0	-0.469200	-3.161075	0.137211
24	1	0	-3.011999	-2.588513	0.115206
25	6	0	-2.487308	-0.473910	0.011578
26	6	0	-3.763486	0.195985	-0.017786
27	6	0	-4.028547	1.553473	-0.101011
28	16	0	-5.265373	-0.712229	0.054847
29	6	0	-5.414294	1.858896	-0.106350
30	1	0	-3.251215	2.307882	-0.157582
31	6	0	-6.203296	0.737220	-0.027613
32	1	0	-5.812477	2.865163	-0.166296
33	1	0	-7.283868	0.677237	-0.012914

Sum of electronic and thermal Free Energies= -1468.902896 au

B3LYP/6-311+G(d,p) geometries (cartesian coordinates) and energies (atomic unit)

Compound **1d**

Center Number	Atomic Number	Atomic Type	Coordinates (Angstroms)		
			X	Y	Z
1	6	0	6.881142	1.210415	0.023789
2	6	0	7.625165	0.059241	0.016311
3	6	0	6.941649	-1.174446	0.002774
4	6	0	5.565899	-1.192384	-0.002481
5	6	0	4.800367	0.004228	0.006005
6	7	0	5.515101	1.192541	0.019053
7	1	0	7.495451	-2.107921	-0.004316
8	1	0	7.336268	2.193122	0.034024
9	1	0	8.706685	0.118480	0.020478
10	1	0	5.044791	-2.140764	-0.014745
11	6	0	3.372663	0.040147	0.000951
12	6	0	2.558700	-1.075106	-0.002580
13	1	0	2.891336	1.009522	-0.000158
14	1	0	3.003472	-2.067785	0.001072
15	6	0	4.809248	2.488015	0.028611
16	1	0	4.194970	2.587749	-0.869494
17	1	0	4.182093	2.567182	0.919788
18	1	0	5.548067	3.287425	0.043108
19	6	0	1.149455	-1.090551	-0.009126
20	6	0	0.337891	-2.232678	-0.011364
21	16	0	0.137963	0.359415	-0.016807
22	6	0	-1.030858	-1.967084	-0.020067
23	1	0	0.757314	-3.233648	-0.007987
24	1	0	-1.792028	-2.738664	-0.025327
25	6	0	-1.338657	-0.596650	-0.023952
26	6	0	-2.618103	0.019358	-0.031105
27	6	0	-2.949739	1.371312	-0.046427
28	16	0	-4.098036	-0.958830	-0.010525
29	6	0	-4.324042	1.643546	-0.045447
30	1	0	-2.198424	2.154467	-0.055699
31	6	0	-5.108820	0.481140	-0.043116
32	1	0	-4.736994	2.643104	-0.044790
33	7	0	-6.459064	0.386726	-0.075851
34	6	0	-7.250849	1.610291	0.045141
35	1	0	-8.294779	1.374709	-0.163234
36	1	0	-7.178257	2.043406	1.051853
37	1	0	-6.915479	2.351622	-0.685613
38	6	0	-7.118740	-0.899465	0.131127
39	1	0	-7.076947	-1.216904	1.182384
40	1	0	-8.163250	-0.816182	-0.171057
41	1	0	-6.649608	-1.669128	-0.489649

Sum of electronic and thermal Free Energies= -1602.820086 au

ⁱ Gaussian 03, Revision E.01, M. J. Frisch, G. W. Trucks, H. B. Schlegel, G. E. Scuseria, M. A. Robb, J. R. Cheeseman, J. A. Montgomery, Jr., T. Vreven, K. N. Kudin, J. C. Burant, J. M. Millam, S. S. Iyengar, J. Tomasi, V. Barone, B. Mennucci, M. Cossi, G. Scalmani, N. Rega, G. A. Petersson, H. Nakatsuji, M. Hada, M. Ehara, K. Toyota, R. Fukuda, J. Hasegawa, M. Ishida, T. Nakajima, Y. Honda, O. Kitao, H. Nakai, M. Klene, X. Li, J. E. Knox, H. P. Hratchian, J. B. Cross, V. Bakken, C. Adamo, J. Jaramillo, R. Gomperts, R. E. Stratmann, O. Yazyev, A. J. Austin, R. Cammi, C. Pomelli, J. W. Ochterski, P. Y. Ayala, K. Morokuma, G. A. Voth, P. Salvador, J. J. Dannenberg, V. G. Zakrzewski, S. Dapprich, A. D. Daniels, M. C. Strain, O. Farkas, D. K. Malick, A. D. Rabuck, K. Raghavachari, J. B. Foresman, J. V. Ortiz, Q. Cui, A. G. Baboul, S. Clifford, J. Cioslowski, B. B. Stefanov, G. Liu, A. Liashenko, P. Piskorz, I. Komaromi, R. L. Martin, D. J. Fox, T. Keith, M. A. Al-Laham, C. Y. Peng, A. Nanayakkara, M. Challacombe, P. M. W. Gill, B. Johnson, W. Chen, M. W. Wong, C. Gonzalez, and J. A. Pople, Gaussian, Inc., Wallingford CT, 2004.